National Défense
Defence nationale

ON THE DESIGN OF FINITE IMPULSE RESPONSE FILTERS FOR PRECISION QUADRATURE DEMODULATION

by

Robert J. Inkol and Ronald H. Saper

DEFENCE RESEARCH ESTABLISHMENT OTTAWA
REPORT N0. 1264

Canada

July 1995
Ottawa

National Defence / Défense nationale

ON THE DESIGN OF FINITE IMPULSE RESPONSE FILTERS FOR PRECISION QUADRATURE DEMODULATION

by

Robert J. Inkol
Electronic Warfare Division

and

Ronald H. Saper
Michel Herzig

DEFENCE RESEARCH ESTABLISHMENT OTTAWA
REPORT N0. 1264

PCN
1410SM/05B02

July 1995
Ottawa

ABSTRACT

The accuracy of digital quadrature demodulation can be improved by optimizing the matching of the in-phase and quadrature channel frequency responses. It is shown that an image rejection ratio exceeding 100 dB can be achieved using a pair of finite impulse response filters having 6 and 5 nonzero coefficients, respectively.

RESUME

La précision de la démodulation numérique en quadrature peut être améliorée en minimisant les différences entre l'amplitude de la réponse en fréquence du filtre dans le canal en phase et celle du filtre du canal en quadrature. Il est montré qu'en utilisant deux filtres à réponse impulsionelle finie ayant chacun 6 et 5 coefficients différents de zéro, on peut réaliser un rapport d'atténuation de fréquence image qui excède 100 dB.

EXECUTIVE SUMMARY

In coherent radar, communication and electronic warfare systems, it is often useful to form the in-phase (I) and quadrature (Q) components of a bandpass signal after it has been shifted to a convenient intermediate frequency (IF). The classical analog quadrature demodulation approach has the problem that accurate amplitude and phase matching of the in-phase and quadrature channels cannot be easily achieved. Consequently, digital approaches for performing quadrature demodulation on a digitized IF signal have attracted attention.

The accuracy of a digital quadrature demodulator is dependent on the matching of the frequency responses and relative phase shifts of the I and Q filters. Finite impulse response filters are attractive since well-known design methods exist which avoid undesired phase mismatches or nonlinearity. However, in quadrature demodulator designs where the constraint $f_s=4f_{IF}$ is used to reduce computational cost, the I and Q filters usually require odd and even numbers of coefficients, respectively. This generally results in mismatches in the frequency responses that can greatly affect performance parameters such as phase error and the image rejection ratio. One solution is to use enough coefficients to achieve a low pass band ripple. This ensures good matching within the specified pass band but may require a large number of coefficients. A more efficient solution is to use a design approach which considers the relative matching of the frequency responses of the I and Q filters. The results presented in this paper for a practical quadrature demodulator confirm that this concept can be realized for filters having a relatively small number of coefficients and that significant performance benefits can be obtained over the full quadrature demodulator bandwidth ($f_s/4$). They provide some useful insights for making tradeoffs in designing digital quadrature demodulators for practical applications. It is also shown that some plausible filter design methods, such as the Hamming window design method, result in inferior performance and should be avoided.

TABLE OF CONTENTS

LIST OF FIGURES

LIST OF FIGURES

1.0 INTRODUCTION

In coherent radar, communication and electronic warfare systems, it is often useful to form the in-phase (I) and quadrature (Q) components of a bandpass signal after it has been shifted to a convenient intermediate frequency (IF). The classical analog quadrature demodulation approach has the problem that accurate amplitude and phase matching of the in-phase and quadrature channels cannot be easily achieved [1]-[2]. Another error results from DC offsets introduced during the analog-to-digital conversion of the I and Q signals. These errors are particularly serious in coherent radar systems. For example, gain and phase errors introduce spurious sidebands at the image Doppler frequency [2]. Consequently, digital approaches for performing quadrature demodulation on a digitized IF signal have attracted attention. Problems with the matching of analog components are eliminated and it is straightforward to achieve high accuracy with filters having a sufficiently large number of coefficients. However, the computational cost can be a significant disadvantage when wideband signals must be processed in real-time.

This problem has motivated the development of digital quadrature demodulation algorithms designed for low computational cost [3]-[5]. These also have significant deficiencies. Approaches based on Hilbert transformers (e.g., [5]) don't suppress DC offsets and require selective analog IF filters since the quadrature demodulator does not have usable stop bands. If infinite impulse response filters are used, as proposed in [4], there are difficulties with the frequency dependence of the group delay.

A recently proposed digital quadrature demodulation algorithm [6] is attractive since it avoids these problems and is computationally efficient. This algorithm, shown in Figure 1, employs a pair of finite impulse response (FIR) highpass filters whose phase shifts differ by $\pi/2$ radians. The even and odd samples of a bandpass signal nominally centered on an intermediate frequency of f_{IF} and sampled at a rate $f_s=4f_{IF}$ are separately processed by the I and Q filters. The decimation operations reduce the output data rate in each channel to $f_s/4$ and result in the highpass output signals from the filters aliasing to baseband without the need for explicit mixing. Consequently, the usable quadrature demodulator bandwidth for which aliasing distortion is avoided is $f_s/4$ centered on f_{IF}.

The coefficients of the I and Q filters, $\{h_m^I\}$ and $\{h_m^Q\}$ respectively, can be obtained from the coefficients of a prototype lowpass filter having N coefficients $\{h_n^P\}$ by

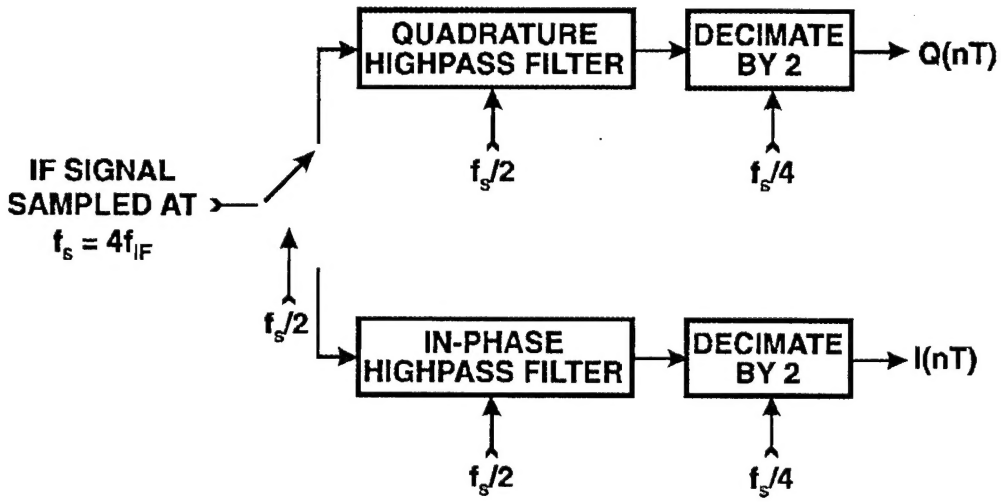

Figure 1. Block diagram of quadrature demodulation algorithm.

$$h_k^I = -2 \cos k\pi \; h_{2k}^P, \qquad 0 \le k \le (N-1)/2$$

$$h_k^Q = 2 \sin (k+1/2)\pi \; h_{2k+1}^P, \qquad 0 \le k \le (N-3)/2 \tag{1}$$

where N-1 *is divisible by* 4,

or

$$h_k^I = 2 \cos k\pi \; h_{2k+1}^P, \qquad 0 \le k \le (N-3)/2$$

$$h_k^Q = -2 \sin (k+1/2)\pi \; h_{2k}^P, \qquad 0 \le k \le (N-1)/2 \tag{2}$$

where N+1 *is divisible by* 4.

These two cases differ in whether the I filter is longer or shorter than the Q filter by one coefficient.[1] The relationship of this quadrature demodulator to approaches employing quadrature mixing and lowpass filtering is discussed in [6]. A similar approach has been advocated for the related problem of designing a complex filter to produce a discrete analytic signal from a discrete real-valued signal [7].

By selecting a quarter-band filter [8] to be the prototype filter, a significant advantage can be obtained in computational efficiency. The bandwidth of the I and Q filters is matched to the output data rate of $f_s/4$ resulting from the decimation operations. Furthermore, for a quarter-band filter

$$h_n^{P4} = 1/4 \; for \; n = (N-1)/2 \tag{3}$$

and

$$h_{4m+q}^{P4} = 0 \; for \; 0 \le m \le INT[(N-1)/4] \; and \; 4m+q \ne (N-1)/2, \tag{4}$$

---

[1] Note that in the second case (i.e., N+1 is divisible by 4) it is necessary to delay the output of the in-phase filter by one sample for correct operation of the quadrature demodulator.

where *INT* means "integer value of" and $q=(mod_8(N-1))/2$. Consequently, the number of multiplications and additions is reduced by nearly 1/4. Note that $q=0$ results in a trivial case where $h_0=h_{N-1}=0$.

The choice of a quarter-band prototype filter results in the I filter being a half-band filter. Half-band filters have symmetrical pass and stop bands with equal ripple. Consequently, the I channel of the quadrature demodulator has an attenuation of 6 dB at $f_s/8$ and $3f_s/8$. The quarter-band stop bands of [DC, $f_s/8$] and [$3f_s/8$, $f_s/2$] relax the stop band attenuation requirements of the analog IF filter, suppress DC offsets from the ADC and reduce quantization noise by approximately 3 dB.

Although the I and Q filters are derived from a common prototype filter, they have a different number of coefficients and their frequency responses do not exactly match as is shown by the frequency responses plotted for the three pairs of quadrature demodulation filters in Figure 2. The matching of the frequency responses is very important because it determines the phase error/image suppression performance [2], [9]. This paper extends the work reported in [6] to show that very good matching of the I and Q filter frequency responses can be achieved with a relatively small number of filter coefficients by the choice of an appropriate filter design method.

2.0 EFFECTS OF FILTER DESIGN PARAMETERS

We have carried out a systematic investigation into the behavior of the quadrature demodulator performance for the most common filter design methods. These include window methods which involve multiplying the time domain coefficients obtained from a Fourier series expansion of the desired frequency response with a window function, and the Remez exchange method. For each design method, quarter-band prototype filters having odd numbers of coefficients up to a maximum of 49 were designed. The performance of the quadrature demodulator was measured for each pair of filters. Performance parameters measured included phase error and, in selected cases, the image rejection ratio and the distortion when used in a frequency demodulator for simulated signals having frequency modulation.

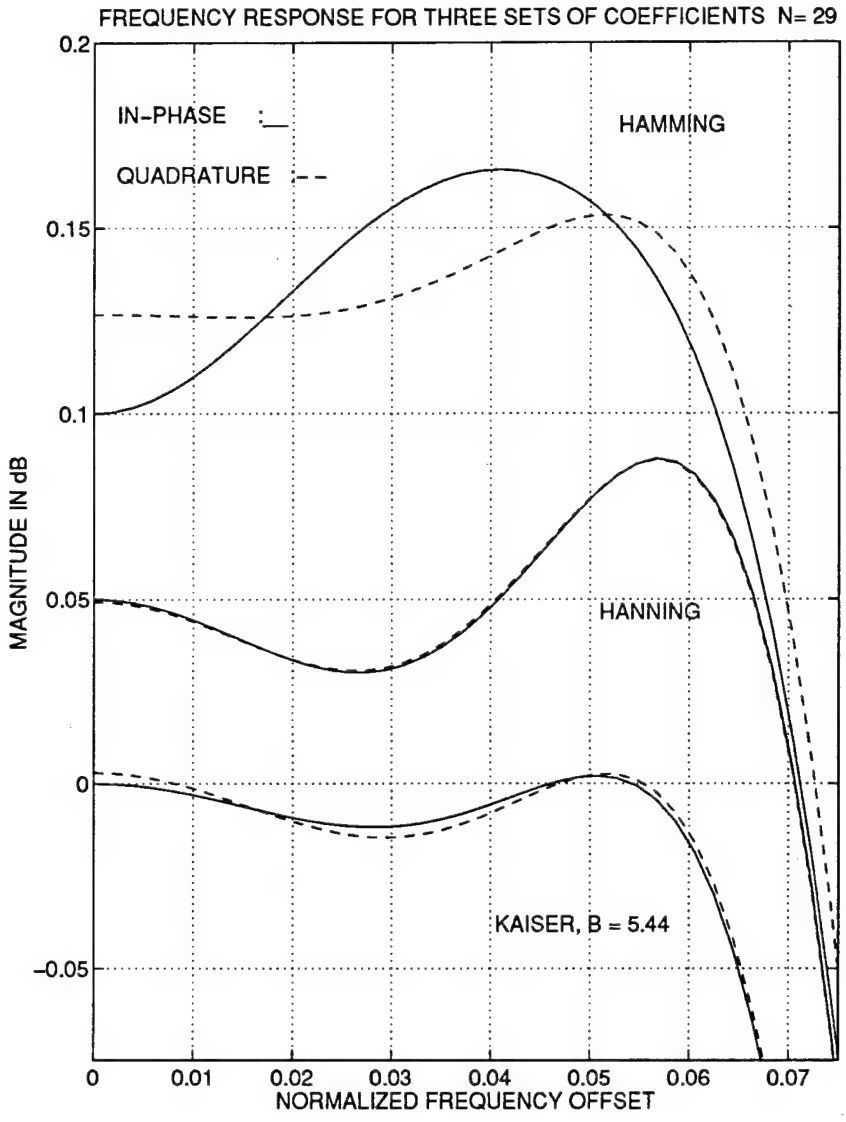

Figure 2: Single sided passband frequency responses of I and Q filters derived from 29 coefficient prototype filters designed using the Hamming, Hanning and Kaiser window methods. The plotted lines for the Hanning and Kaiser windows are intentionally offset by -0.05dB and -0.1 dB, respectively. The horizontal scale is normalized to f_s.

A. Phase Error Performance - Window Design Methods

The MATLAB™ *fir2* function was used to design the quarter-band lowpass prototype filters by setting the pass band bandwidth to $f_s/8$. The phase error performance was investigated for one and two term cosine windows and the Kaiser and Chebyshev windows. The Kaiser [10] and Chebyshev [11] windows each have an adjustable parameter, B and R, respectively, that can be set to provide a tradeoff between the mainlobe width and sidelobe levels of the window. To implement these windows, we used the MATLAB *kaiser* and *chebwin* functions.

From each prototype filter a pair of I and Q filters was constructed and their frequency responses determined at 64 discrete frequencies distributed over the bandwidth $[f_s/8, f_s/4]$. It is not necessary to compute them over the full bandwidth $[f_s/8, 3f_s/8]$ since the frequency responses of the I and Q filters are symmetric about $f_s/4$. The phase error bound [9] was computed using

$$\phi_e(f_i)=\arctan(|Q(f_i)|/|I(f_i)|)-\pi/4, \tag{5}$$

where $Q(f_i)$ and $I(f_i)$ are the magnitudes of the frequency responses of the Q and I channels at a discrete frequency f_i. In the time domain, the phase error will oscillate between $-\phi_e(f_i)$ and $+\phi_e(f_i)$ with a frequency $2|f_i-f_s/4|$. For small values of $\phi_e(f_i)$, the RMS value of the phase error at f_i, will be approximately $\phi_e(f_i)/\sqrt{2}$. Using this result, a measure of the performance for all f_i is provided by the RMS phase error ϕ_{rms} given by

$$\phi_{rms}=\left[\sum_{i=1}^{I}\phi_e(f_i)^2/2I\right]^{1/2}, \tag{6}$$

where I is the number of discrete frequencies. Although this approach is an indirect way of measuring the phase error, we have found good agreement with direct measurements of the phase error of the quadrature demodulator algorithm for simulated sinusoidal signals.

Figures 3 and 4 plot the RMS and peak phase errors for the rectangular and cosine windows as a function of the number of coefficients used in the prototype filter. The Hamming window, although better than a rectangular (boxcar) window, has a poor performance and its general trend shows only a slow improvement with an increasing number of coefficients. The phase error for the Hanning window is considerably better and its trend with respect to the number of coefficients shows a steeper slope. The Blackman window shows a further improvement. A rather different behavior is observed for the Kaiser and Chebyshev windows plotted in Figures

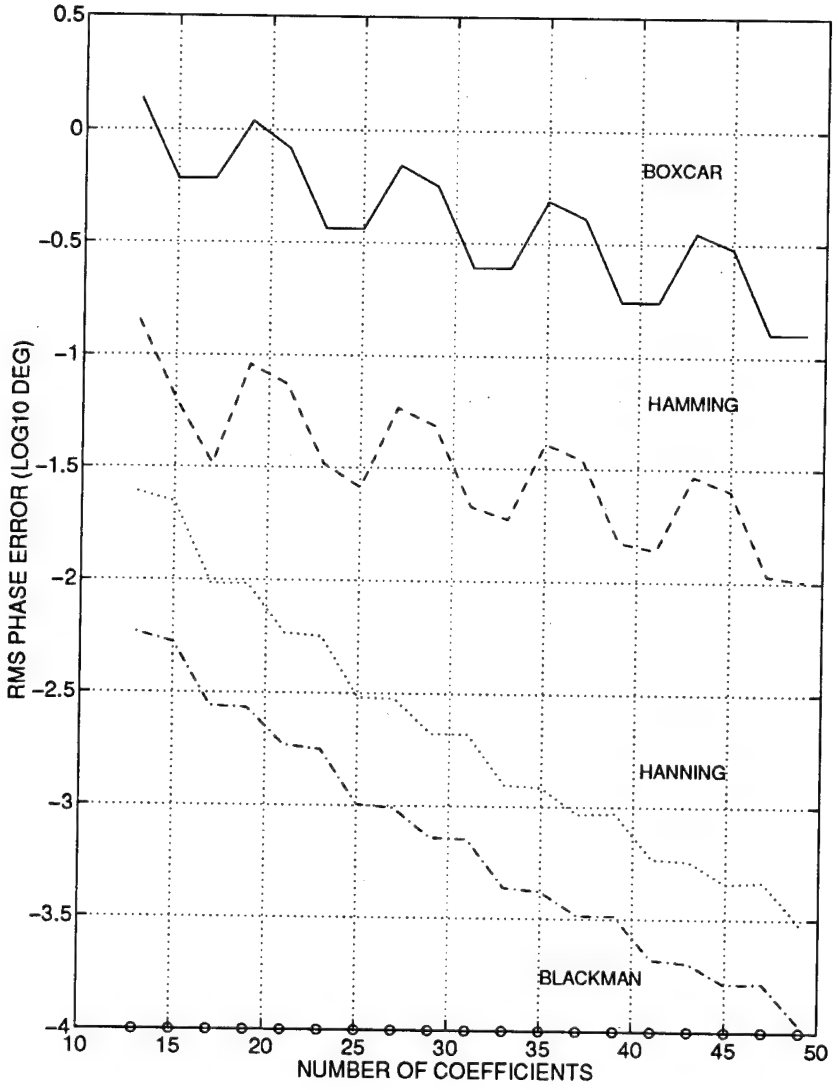

Figure 3: RMS phase error over bandwidth of [$f_s/8$, $3f_s/8$] plotted as a function of the number of coefficients for quadrature demodulation filters derived from prototype filters designed using rectangular and common cosine windows.

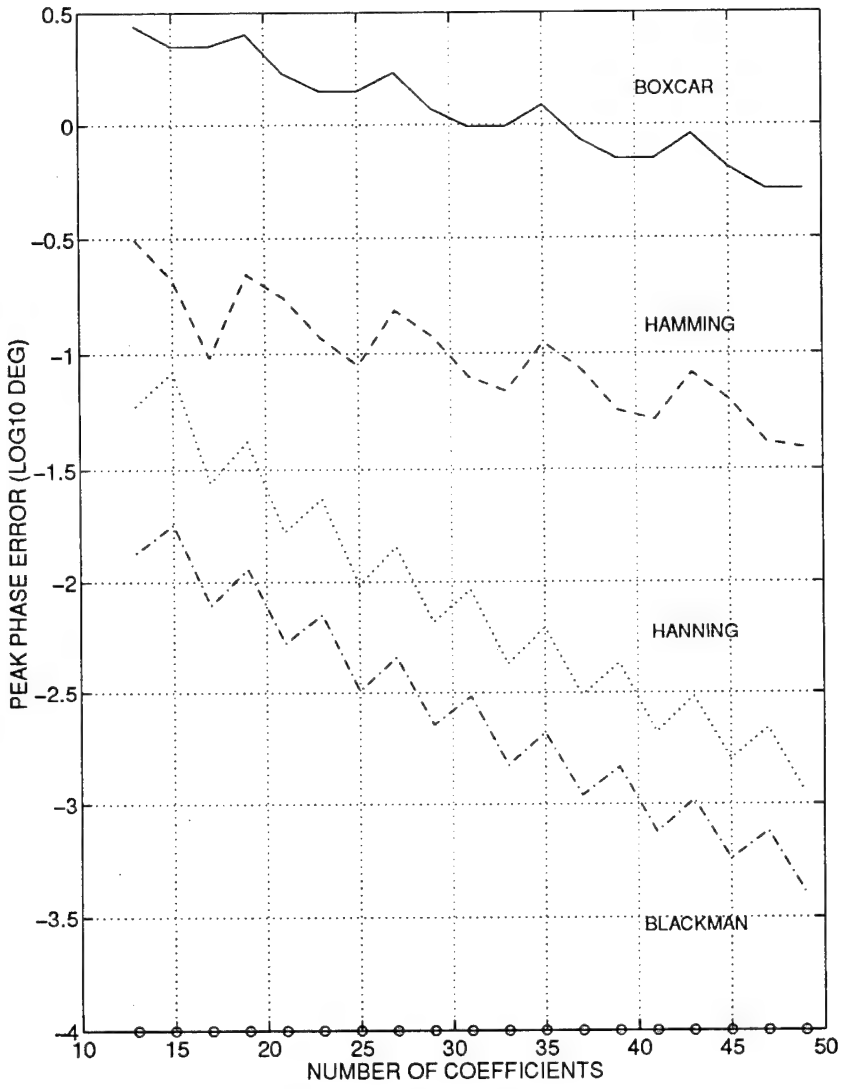

Figure 4: Peak phase error over bandwidth of $[f_s/8, 3f_s/8]$ plotted as a function of the number of coefficients for quadrature demodulation filters derived from prototype filters designed using rectangular and common cosine windows.

5 and 6. The phase error rapidly decreases as the number of coefficients increases and then fluctuates around a value that is largely determined by the window parameters B and R, respectively and has only a weak dependence on the number of coefficients.

Appendix A presents additional results including graphs of the I and Q filter frequency responses and phase error bounds for some filter design examples.

B. Phase Error Performance - Remez Exchange Method

The Remez exchange method in the form of the computer program of McClellan and Parks [12] is one of the most widely used iterative approaches for designing FIR filters. It is an optimal method in the sense that it minimizes the maximum absolute error in the frequency response for the chosen pass and stop band specifications. However, it is not possible to provide a frequency response specification that will directly result in a fractional band filter where the appropriate coefficients have values of zero. A procedure has been proposed in [8] for designing fractional band FIR filters using the McClellan and Parks program. For a quarter-band filter, the filter specification is set to satisfy the conditions

$$f_1 + f_2 = 0.25 f_s \quad \textit{and} \quad W_1 = 3W_2. \tag{7}$$

where f_1 and f_2 are the pass band and stop band cutoff frequencies, respectively, and W_1 and W_2 are the weights to be given to the pass and stop band errors, respectively. In the resultant filter the coefficients, which should be zero, are small, but not zero. A quarter-band filter is then derived by directly modifying coefficients to satisfy (3)-(4). This filter is known to be suboptimal in that the sidelobe levels are slightly degraded.

Four families of I and Q filters were derived from lowpass prototype filters designed using the MATLAB *remez* function, and selecting the cutoff frequencies of the pass and stop bands to result in transition bands having widths of $0.075f_s$, $0.125f_s$, $0.175f_s$, and $0.225f_s$, respectively. The phase error results obtained for these quarter-band filters were very poor, in most cases the peak phase error exceeded one degree. It was determined that the matching of the frequency responses of the I and Q filters was generally very poor outside the pass band. Additional results were obtained for filters with unmodified coefficients. These results were considerably better and are plotted in Figures 7 and 8. The performance improves as both N and the width of the transition band (f_2-f_1) increase. We also tried an alternative approach in which the I and Q filters were separately designed using the common design specifications

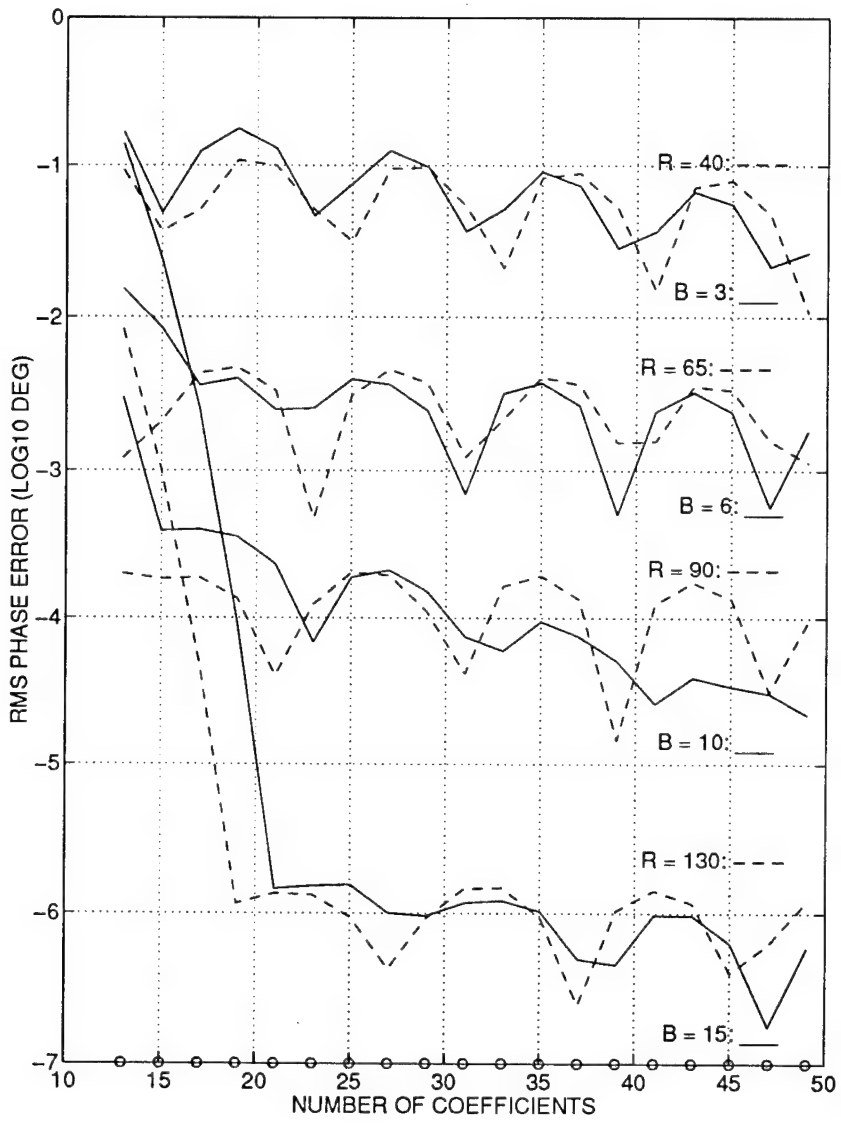

Figure 5: RMS phase error over bandwidth of $[f_s/8, 3f_s/8]$ plotted as a function of the number of coefficients for quadrature demodulation filters derived from prototype filters designed using Kaiser and Chebyshev windows. B and R are the design parameters for the Kaiser and Chebyshev windows, respectively.

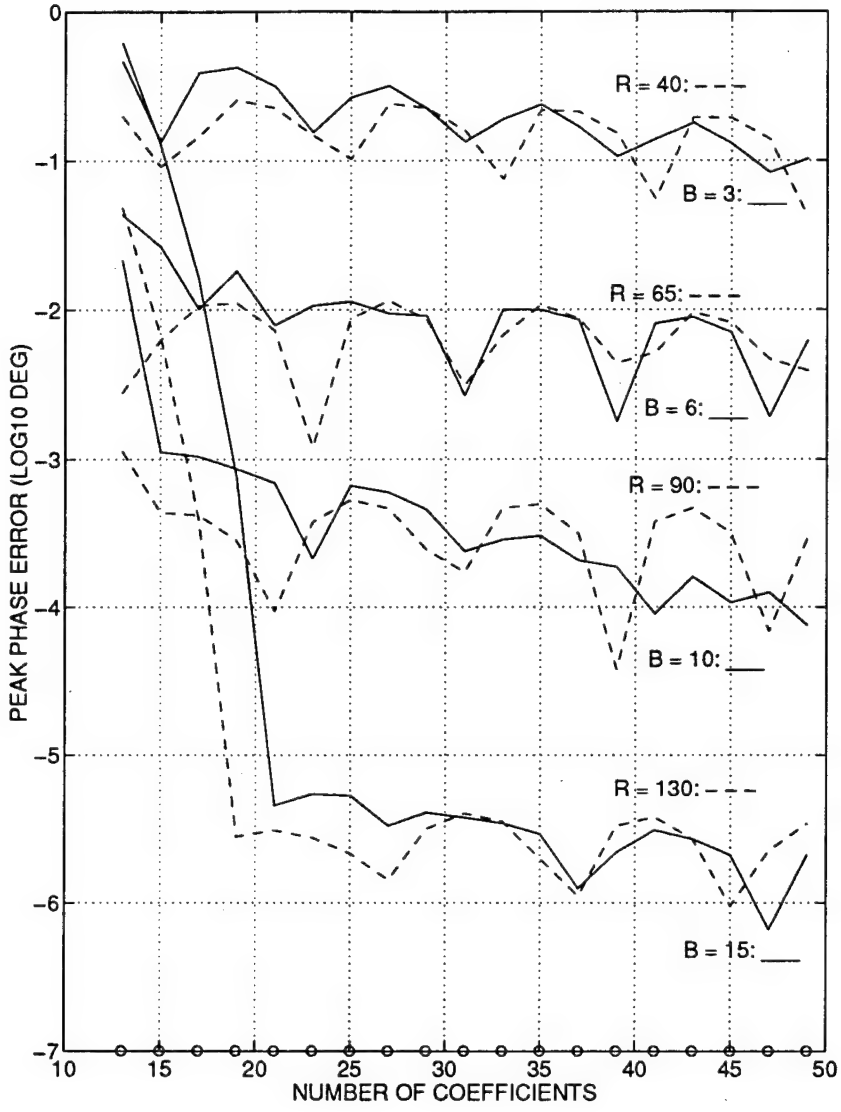

Figure 6: Peak phase error over bandwidth of $[f_s/8, 3f_s/8]$ plotted as a function of the number of coefficients for quadrature demodulation filters derived from prototype filters designed using Kaiser and Chebyshev windows. B and R are the design parameters for the Kaiser and Chebyshev windows, respectively

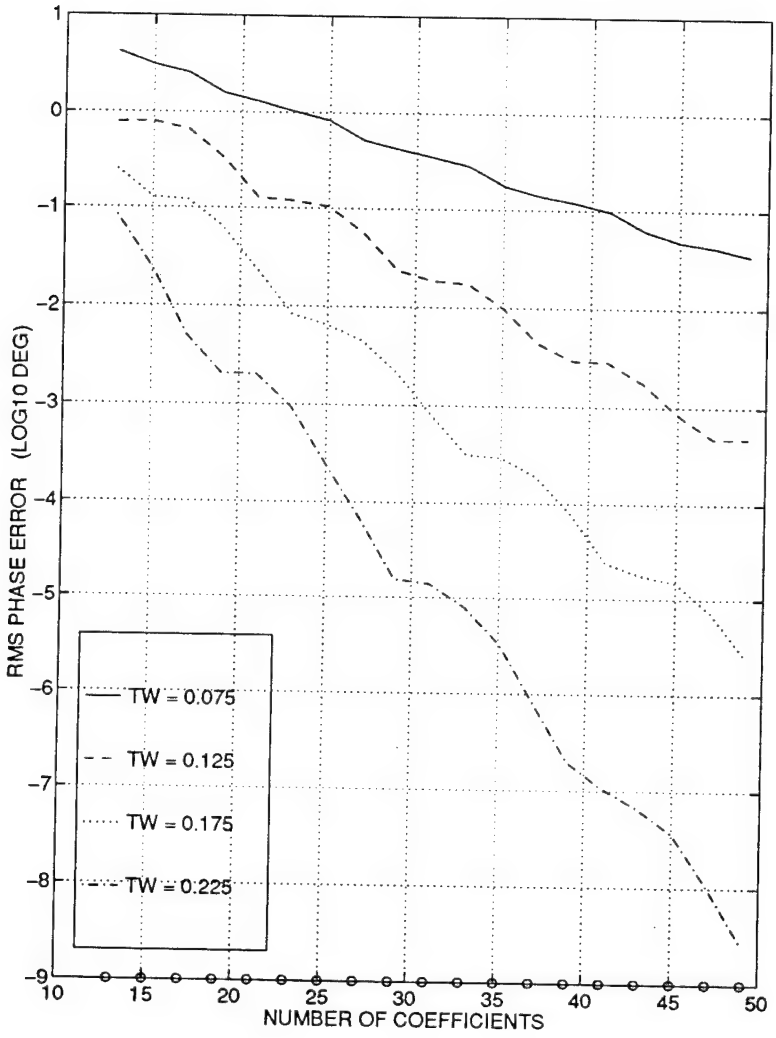

Figure 7: RMS phase error over bandwidth of $[f_s/8, 3f_s/8]$ plotted as a function of the number of coefficients for quadrature demodulation filters derived from prototype filters designed using Remez exchange method. TW specifies the transition bandwidth of the prototype filter normalized to f_s.

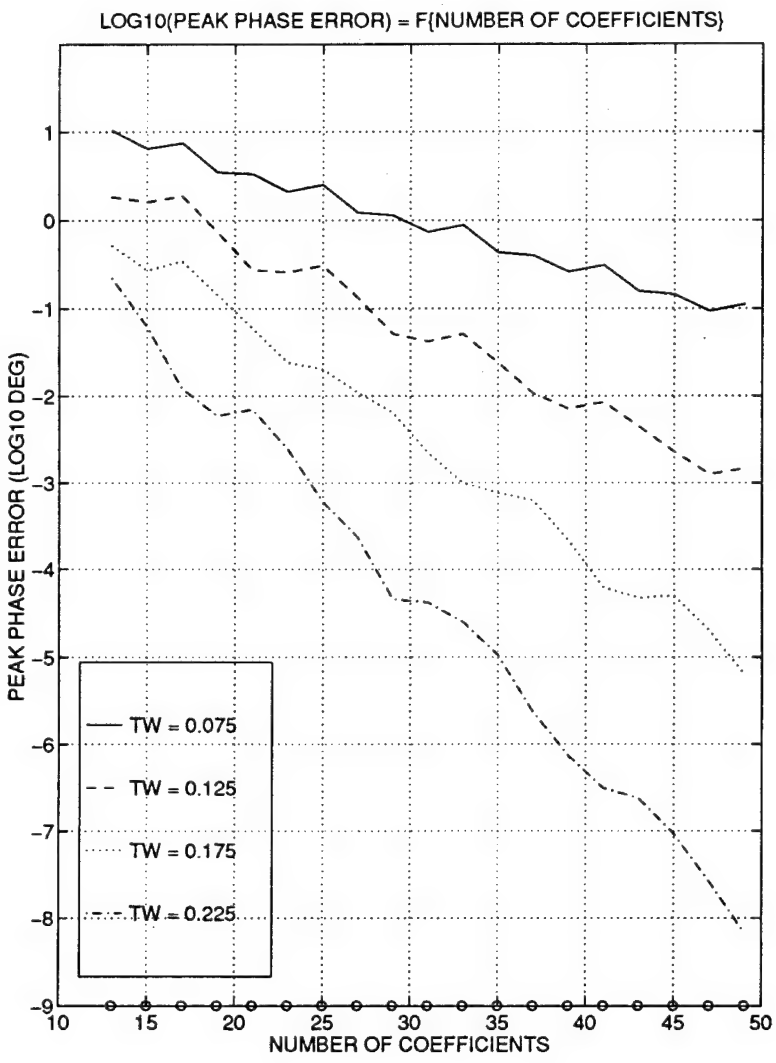

Figure 8: Peak phase error over bandwidth of $[f_s/8, 3f_s/8]$ plotted as a function of the number of coefficients for quadrature demodulation filters derived from prototype filters designed using Remez exchange method. TW specifies the transition bandwidth of the prototype normalized to f_s.

$$f_1 + f_2 = 0.5 f_s \quad and \quad W_1 = W_2. \tag{8}$$

These parameters are consistent with the I filter being a half-band filter. The phase error performance was inferior to that obtained when the filters were derived from a quarter-band prototype filter designed using the Remez exchange method without modifying filter coefficients to satisfy (3)-(4).

C. Image Rejection Ratio Results

Another performance parameter of interest is the image rejection ratio. For a sinusoidal input signal, the expected output signal of a quadrature demodulator has a spectral component at a frequency corresponding to the frequency offset of the input signal from the center frequency of the quadrature demodulator (f_{IF}). The ratio of the power in this spectral component to the spurious image at the negative frequency is the image rejection ratio.

The image rejection ratios were measured for quadrature demodulation filters designed using the Hamming, Hanning and Chebyshev design methods at frequency offsets of 0.00195 f_s, 0.03125f_s, 0.0625f_s and 0.09375f_s from $f_s/4$. The powers contained in the signal and negative image components were computed from the power spectrum of the I and Q signals obtained by using a 512 point complex FFT. A window was not used with the FFT since problems with spectral leakage were avoided by selecting the period of the modulating signal to be an exact multiple of the FFT duration. Table I presents the results for the test signals.

D. Distortion Performance - Frequency Demodulation

Some investigations were carried out concerning the effects of different windows on the distortion performance achieved with the quadrature demodulator when used in an FM demodulator. FM demodulation was performed by generating a sequence of phase data by computing the 4 quadrant arctangent of $(Q(jT)/I(jT))$, unwrapping the phase data by using the MATLAB *unwrap* function and differentiating the unwrapped phase data by using a 5 point Lagrange differentiator. The signal power and total power were then computed from the power spectrum of the demodulated signal obtained by using a 512 point FFT. A window was not used with the FFT since problems with spectral leakage were avoided by selecting the period of the modulating signal to be an exact multiple of the FFT duration. Tables II and III give the peak spurious signal and, between parenthesis, distortion to signal power + distortion ratios for the demodulated signal where the input signal is frequency modulated by a sinusoid of frequency 0.0004883f_s with a frequency deviation of ±0.0025f_s and ±0.05f_s, respectively.

Table I: Image Rejection Ratio for Sinusoid Signal Offset In Frequency from Quadrature Demodulator Center Frequency.

	$F_{off} = \pm 0.00195 f_s$	$F_{off} = \pm 0.03125 f_s$	$F_{off} = \pm 0.0625 f_s$	$F_{off} = \pm 0.09375 f_s$
Hamming (N=13)	47.8 dB	56.9 dB	48.8 dB	45.7 dB
Hanning (N=13)	66.4 dB	73.5 dB	65.6 dB	59.7 dB
Cheb. (N=13, R=90)	108.1 dB	115.4 dB	109.0 dB	104.1 dB
Hamming (N=29)	56.3 dB	56.6 dB	57.6 dB	58.5 dB
Hanning (N=29)	88.0 dB	88.2 dB	88.9 dB	89.6 dB
Cheb. (N=29, R=200)	141.6 dB	142.1 dB	143.3 dB	145.1 dB

Table II. Peak Spurious Signal to Signal and, between parenthesis, Total Distortion to Signal + Distortion ratios for demodulated signal having sinusoidal frequency modulation (frequency excursion =±0/0025f_s, frequency of modulating signal = 0.0004883f_s).

Number of Coeff.	Hamming	Hanning	Chebyshev
13	-47.3 dB (-44.8 dB)	-65.8 dB (-63.3 dB)	-77.1 dB (-74.5 dB) R=60
29	-55.9 dB (-53.4 dB)	-87.6 dB (-85.1 dB)	-121.6 dB (-119.1 dB) R=100
45	-61.8 dB (-59.3 dB)	-100.9 dB (-98.4 dB) dB))	-142.3 dB (-139.7 dB) R=120

Table III. Peak Spurious Signal to Signal and, between parenthesis, Total Distortion to Signal + Distortion ratios for demodulated signal having sinusoidal frequency modulation (Frequency excursion = ±0.05f_s, Frequency of modulating signal = 0.0004883f_s).

Number of Coeff.	Hamming	Hanning	Chebyshev
13	-71.4 dB (-57.3 dB)	-89.3 dB (-75.2 dB)	-96.6 dB (-86.0 dB) R=60
29	-73.4 dB (-60.8 dB)	-103.4 dB (-90.6 dB)	-103.0 dB (-103.0 dB) R=100
45	-78.0 dB (-65.7 dB)	-107.4 dB (-101.7 dB)	-116.7 dB (-114.0 dB) R=120

3.0 DISCUSSION

The phase error results show that the error performance of the quadrature demodulator for signals having a narrow instantaneous bandwidth is dependent on the choice of filter design method. This behavior results from differences in the matching of the frequency responses. For example, the Hanning window has a considerable superiority over the Hamming window and compares well with the Kaiser window having the same mainlobe width (B=5.44) except for filters having a small number of coefficients. The good performance achieved with the Hanning window is a result of the closely matched frequency responses of the I and Q filters although, as can be seen in Figure 2, the Kaiser window has a much lower pass band ripple. While the matching of the frequency responses for the Kaiser window was not as good as for the Hanning window in this example, the Kaiser window is preferable in this respect to the Chebyshev window and can provide a better performance for a given pass band ripple specification.

Very low phase errors can be obtained by trading off the pass band cutoff frequency of the filters for lower pass band ripple by using Kaiser or Chebyshev windows with a large value of B or R, respectively. Furthermore, this is true for the full usable bandwidth ($f_s/4$) of the quadrature demodulator. For example, a pair of I and Q filters having a total of 29 coefficients and designed using a Kaiser window with B=7 can achieve an RMS phase error of 0.0006 degrees over $[f_s/8, 3f_s/8]$, a smaller error than would be expected from the quantization of noiseless signal data to 14 bit resolution. It is interesting to note that an analogous behavior has been observed for Hilbert transformers. Reference 13 advises that the bandwidth of the Hilbert transformer should be made as small as possible (i.e., the width of the transition band should be made as large as possible) for the lowest approximation error. However, unlike the quadrature demodulation algorithm considered in this paper, quadrature demodulation algorithms based on the Hilbert transformer cannot provide a usable performance for frequencies in the transition band(s) since there will be a large mismatch in the frequency responses of the I and Q channels.

It has been observed that low phase errors are generally obtained for windows which smoothly decrease to zero if extrapolated to zero at the sample points immediately outside the window bounds. The Hanning window is a simple example of such a window. Conversely, a window, such as the Hamming window, which has a shape near its edges that approximates a step function is especially poor. A similar behavior can be observed for the Chebyshev window. Unlike most common windows, the shape of the Chebyshev window is dependent on the number of sample points. For low values of R and sufficiently large N, the magnitude of

the Chebyshev window endpoints increases with increasing N.[2] For further increases in N the endpoints can be larger in magnitude than their interior neighbours. The effect of this behavior is apparent in the phase error plotted in Figures 5 and 6 for R=40. There are marked local minima at N=25, 33, 41 and 49. For these values of N the endpoints of the window are immaterial since they correspond to zero valued filter coefficients (i.e., the same result would be obtained by setting the endpoints of the window to zero). Furthermore, we were able to reduce the phase error performance for most values of N greater than 21 by modifying the R=40 Chebyshev window by selecting a window for N+2 points and simply deleting each endpoint. This behavior was not observed for R$\geq$ 60 or for the other windows tested with the exception of the Hamming window. These results suggest that the Chebyshev window is a questionable choice for R<50.

The poor results obtained with quarter-band filters designed using the Remez exchange method with the procedure proposed in [8] result from perturbations in the frequency response of the I filter caused by modifying the coefficients to satisfy (3)-(4). Much better results were obtained when the unmodified coefficients were used.[3] As with the filters designed using window methods, good matching of the frequency responses of the I and Q channels can be obtained by making the transition band width sufficiently large.

The idea of separately designing the I and Q filters, instead of deriving them from a common prototype filter, is questionable. Although the matching of the frequency responses may be acceptable within the pass band if the filters are designed for a low pass band ripple, it may be very poor outside it. This was confirmed by the results obtained when the Remez exchange method was used to separately design the I and Q filters. Since the Remez exchange method does not place any weight on the behaviour of the filters in the transition band, it is not surprising that filters having differing numbers of coefficients have dissimilar frequency responses in the transition band.

The image rejection ratio and frequency demodulation results also confirm the benefit of matching the frequency responses of the I and Q channels. The observed image rejection ratio results are consistent with the theoretical relationship given by

---

[2]Note that this is the opposite of what occurs for the Hanning and Blackman windows or the Chebyshev window for large R.

[3]Note that the prototype filter using the unmodified coefficients is not a true quarter-band filter. Consequently, there is no saving in computational cost resulting from having zero valued coefficients.

$$I_r(f_i) = 10\,Log\frac{1+2E(f_i)+E(f_i)^2}{1-2E(f_i)+E(f_i)^2}, \qquad (9)$$

where $E(f_i)$ is the ratio of gains of the I and Q channels at a frequency f_i and the filters have a relative phase shift of $\pi/2$ [2]. As is the case for the phase error, there is a large variation for different types of windows. It is noteworthy that an image rejection ratio exceeding 100 dB can be obtained with only 13 coefficients, of which 2 have values of zero. The results in Tables II and III show that very low distortion is achievable in the frequency demodulation of signals having wideband FM modulation if a sufficiently high sampling rate is used.

The cost of obtaining a good phase error/image rejection ratio performance with a small number of coefficients is in the size of the transition band between the pass and stop bands of each filter. Since the phase error and image rejection ratio results apply to a sinusoidal signal at a discrete frequency, there is no aliasing distortion and deviations from a flat frequency response near the edges of the quadrature demodulator bandwidth are unimportant. However, in applications involving signals whose instantaneous bandwidth is large or which require high selectivity, it may be necessary to increase the number of coefficients to obtain the desired performance. Nevertheless, quadrature demodulation filters designed for good frequency matching can provide significant benefits in many applications, particularly those where the instantaneous bandwidth of the signal is relatively small.

4.0 CONCLUSIONS

The accuracy of a digital quadrature demodulator is dependent on the matching of the frequency responses and relative phase shifts of the I and Q filters. FIR filters are attractive since well-known design methods exist which avoid undesired phase mismatches or nonlinearity. However, in quadrature demodulator designs where the constraint $f_s=4f_{IF}$ is used to reduce computational cost, the I and Q filters usually require odd and even numbers of coefficients, respectively. This generally results in mismatches in the frequency responses that can greatly affect performance parameters such as phase error and the image rejection ratio. One solution is to use enough coefficients to achieve a low pass band ripple. This ensures good matching within the specified pass band but may require a large number of coefficients. A more efficient solution is to use a design approach which considers the relative matching of the frequency responses of the I and Q filters. The results

presented in this paper for a practical quadrature demodulator confirm that this concept can be realized for filters having a relatively small number of coefficients and that significant performance benefits can be obtained over the full quadrature demodulator bandwidth ($f_s/4$). They provide some useful insights for making tradeoffs in designing digital quadrature demodulators for practical applications. It is also shown that some plausible filter design methods, such as the Hamming window design method and the procedure proposed in [8] for designing Nth band filters with the Remez exchange method result in inferior performance and should be avoided.

5.0 REFERENCES

[1] D.L. Sharpin, J.B.Y. Tsui, J. Hedge, and B. Haber, "The Effects of Quadrature Sampling Imbalances on a Phase Difference Analysis Technique", 1990 National Aerospace Electronics Conference, pp. 962-968, May 1990.

[2] A.I. Sinsky and P.C. Wang, "Error Analysis of a Quadrature Coherent Detector Processor", "IEEE Trans. on Aerospace and Electronic Syst., AES-10, pp. 880-883, Nov. 1974.

[3] R.L. Mitchel, "Creating Complex Signal Samples from a Bandlimited Real Signal", IEEE Trans. on Aerospace and Electronic Syst., AES-25, pp. 425-427, May 1989.

[4] C.M. Rader, "A Simple Method for Sampling In-phase and Quadrature Components", IEEE Trans. on Aerospace and Electronic Syst., VOL. 20, NO. 6, pp. 821-824, Nov. 1984.

[5] W.M. Waters and B.R. Jarret, "Baseband Signal Sampling and Coherent Detection", IEEE Trans. on Aerospace and Electronic Syst., AES-18, pp. 731-736, Nov. 1982.

[6] G. Zhang, D. Al-Khalili, R. Inkol and R. Saper, "Novel Approach to the Design of I/Q Demodulation Filters", IEE Proc. Vis. Image Signal Processing, Vol. 141, No. 3, pp. 154-160, June 1994.

[7] A. Reilly, G. Frazer and B. Boashash, "Analytic Signal Generation-Tips and Traps", IEEE Trans. Signal Process., VOL. 42, No. 11, pp. 3241-3245, Nov. 1994.

[8] F. Mintzer, "On Half-Band, Third-Band, and Nth-Band FIR Filters and their Design", IEEE Trans. Acoust., Speech, Signal Processing, VOL. ASSP-30, NO. 5, pp. 734-738, Oct. 1982.

[9] J. Lee, "Effects of Imbalances and DC offsets on I/Q Demodulators", DREO Report No. 1148, Dec. 1992.

[10] J.F. Kaiser, "Nonrecursive Digital Filter Design Using the I_0-Sinh Window Function", Proc. IEEE Int. Symp. on Circuits and Syst., pp. 20-23, April 1974.

[11] H.D. Helms, "Nonrecursive Digital Filters: Design Methods for Achieving Specifications on Frequency Response", IEEE Trans. Audio, Electroacoust., vol AU-16, pp. 336-342, Sept. 1968.

[12] J.H. McClellan, T.W. Parks and L.R. Rabiner, "A Computer Program for Designing Optimal FIR Linear Phase Filters", IEEE Trans. Audio, Electroacoust., vol. AU-21, pp. 506-526, Dec. 1973.

[13] L.R. Rabiner and R.W. Schafer, "On the Behavior of Minimax FIR Digital Hilbert Transformers", The Bell System Technical Journal, Vol. 53, No. 2, February 1974.

APPENDIX A - PERFORMANCE DATA FOR DESIGN EXAMPLES

A pair of I and Q filters generally have slightly different pass band ripple and stopband attenuation specifications than the prototype lowpass filter from which they were derived. Consequently, to obtain a pair of I and Q filters meeting a given frequency response specification, an iterative search strategy may be required to find a suitable set of filter design parameters for the prototype filter. The availability of frequency response results for various filter design parameters is therefore useful since it may eliminate the need for a search or, if used to provide a good starting point, reduce the number of iterations required. This appendix provides graphical results for pairs of I and Q filters derived from examples of prototype filters designed using the Kaiser window and Remez exchange methods. The results plotted for each example include:

(i) frequency responses of I and Q filters plotted using two different scales;
(ii) frequency response of the prototype lowpass filter;
(iii) the bound for the peak phase error of the quadrature demodulator plotted as a function of frequency.

The results for (i) and (iii) are single sided frequency responses which are plotted as a function of the frequency offset from the quadrature demodulator center frequency. The horizontal scale is normalized to the sampling rate.

KAISER B = 3 N = 29 RES = FLOATING POINT

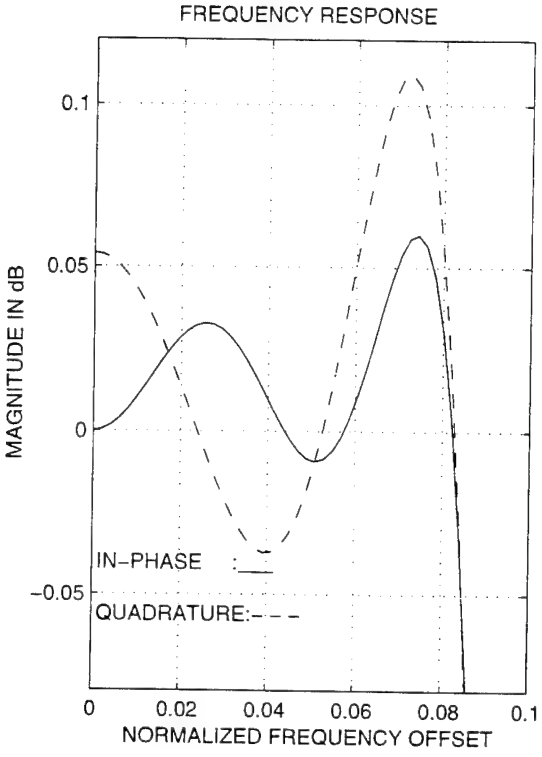

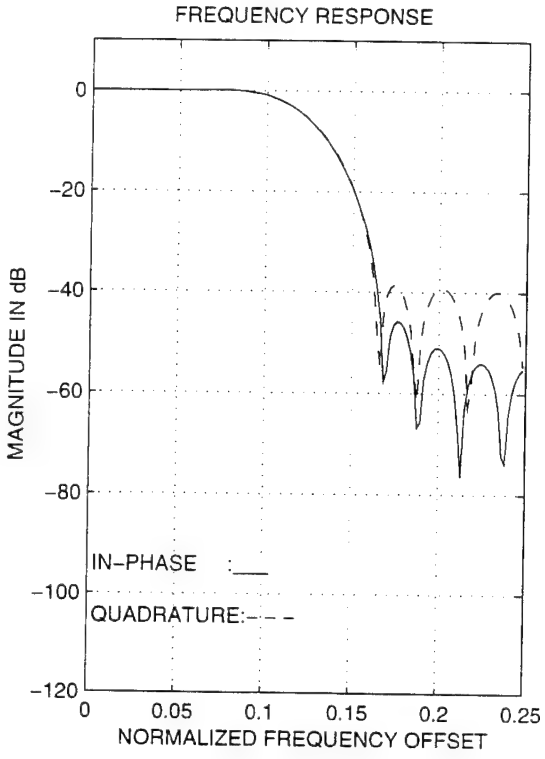

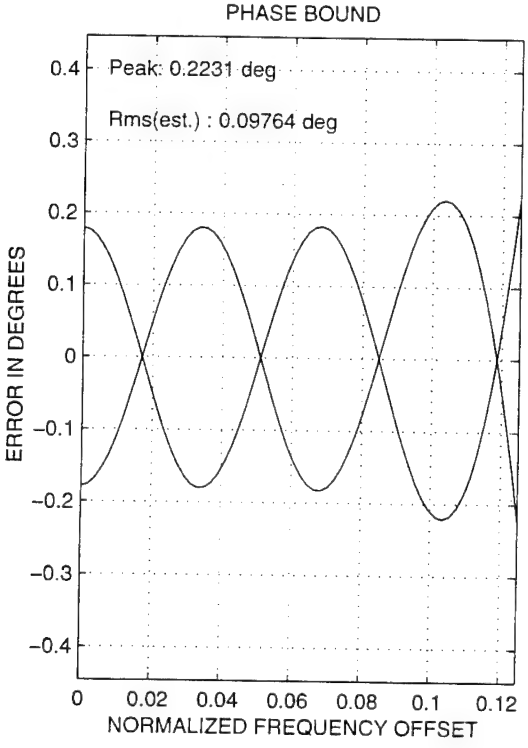

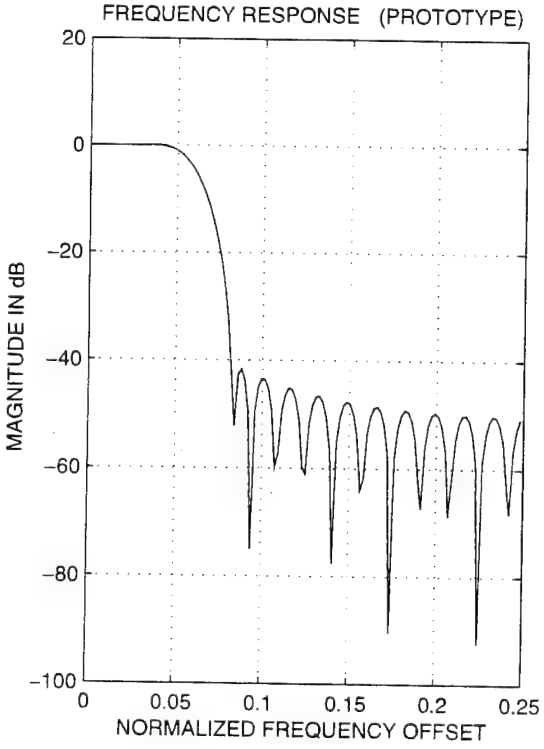

KAISER B = 4 N = 29 RES = FLOATING POINT

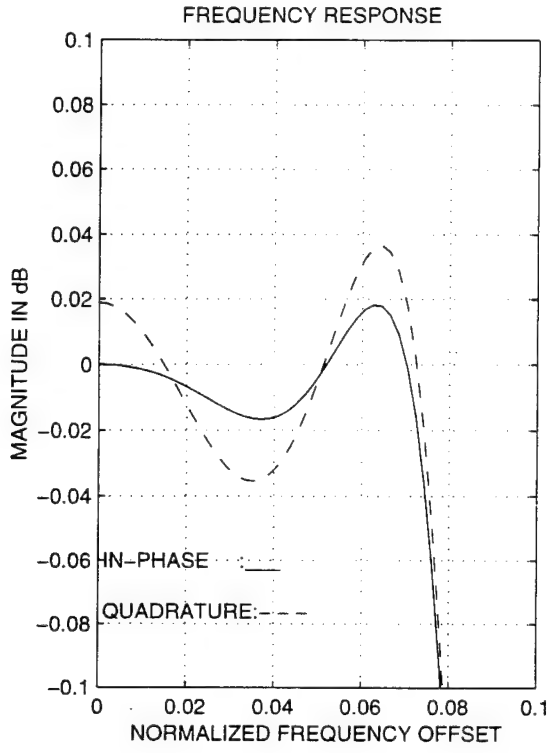

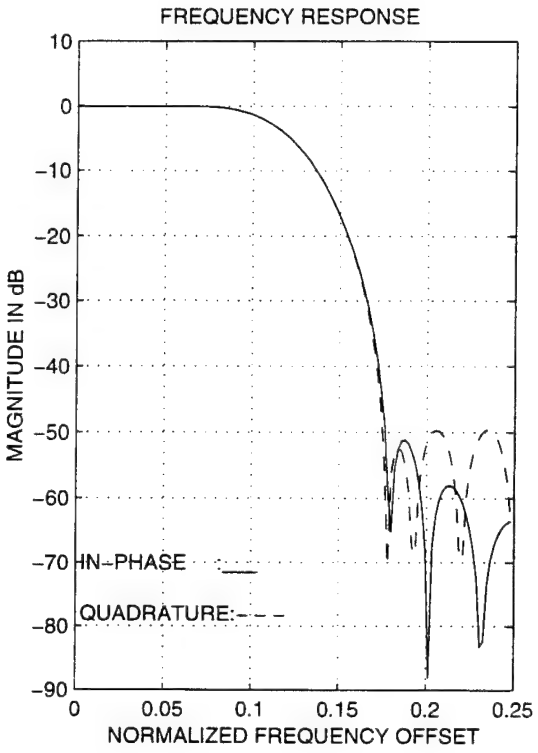

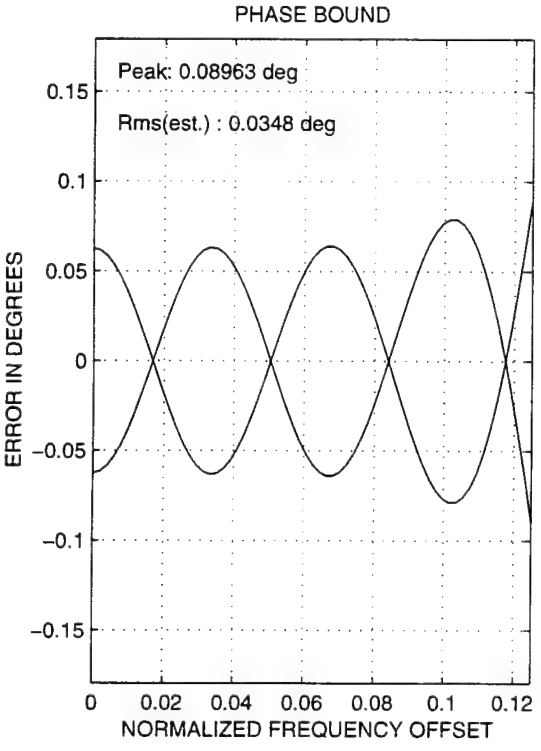

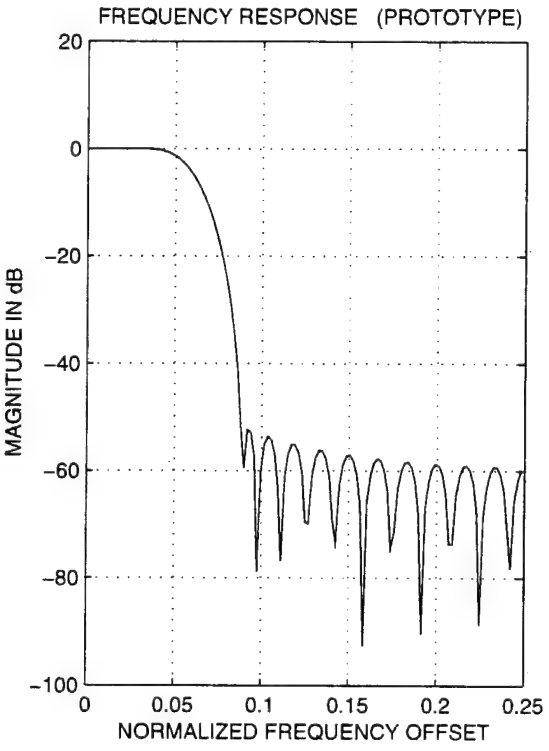

KAISER B = 5 N = 29 RES = FLOATING POINT

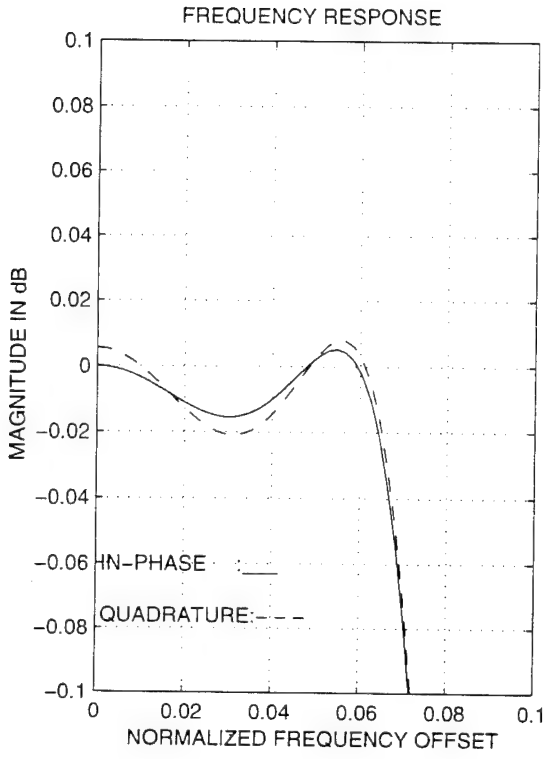

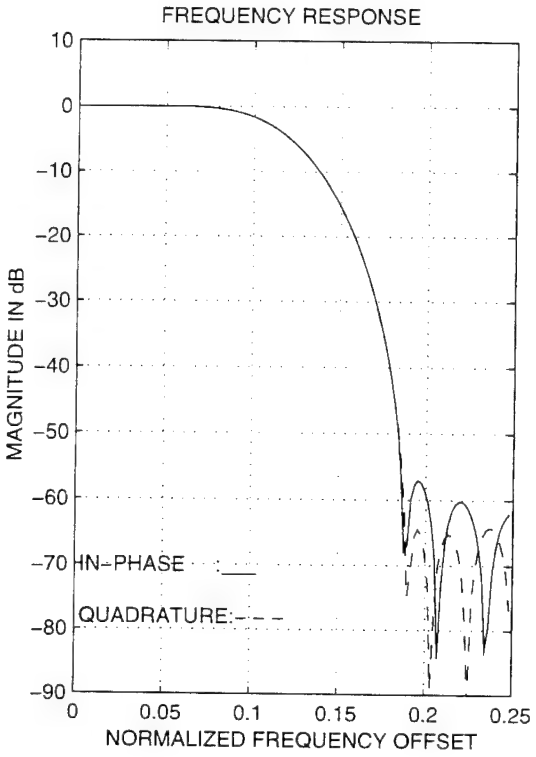

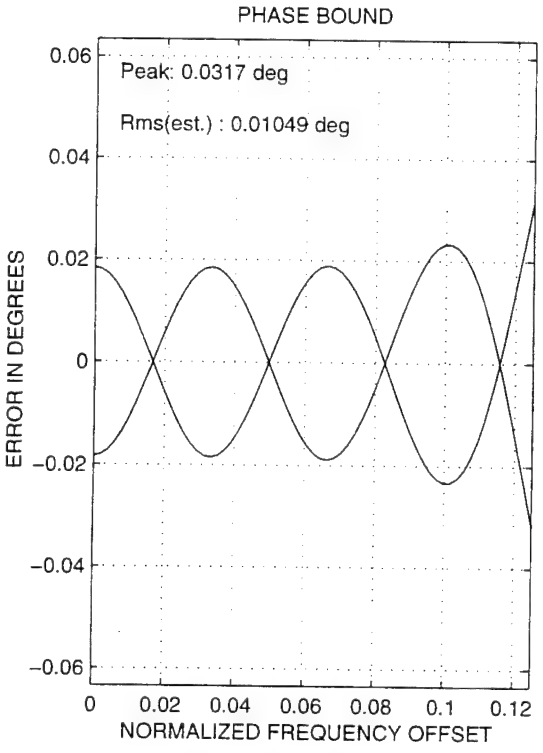

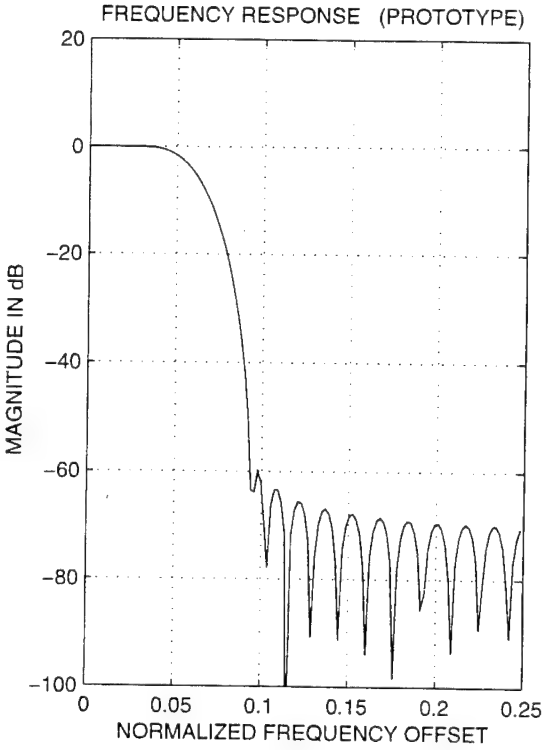

KAISER B = 6 N = 29 RES = FLOATING POINT

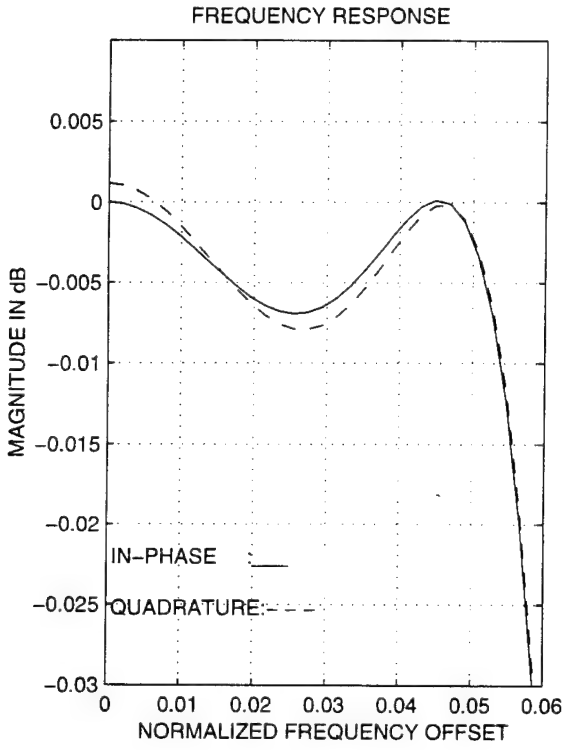

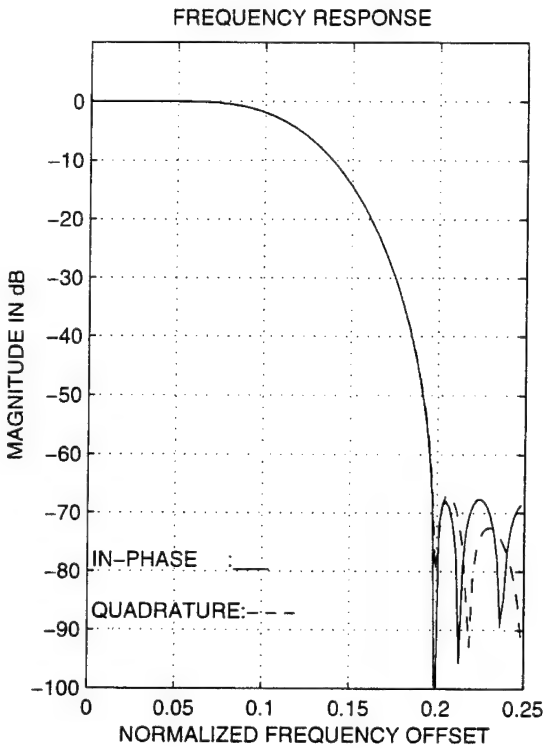

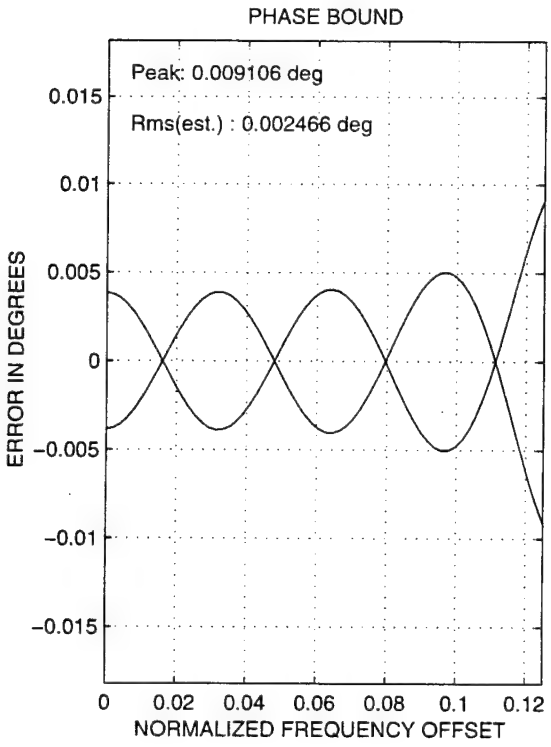

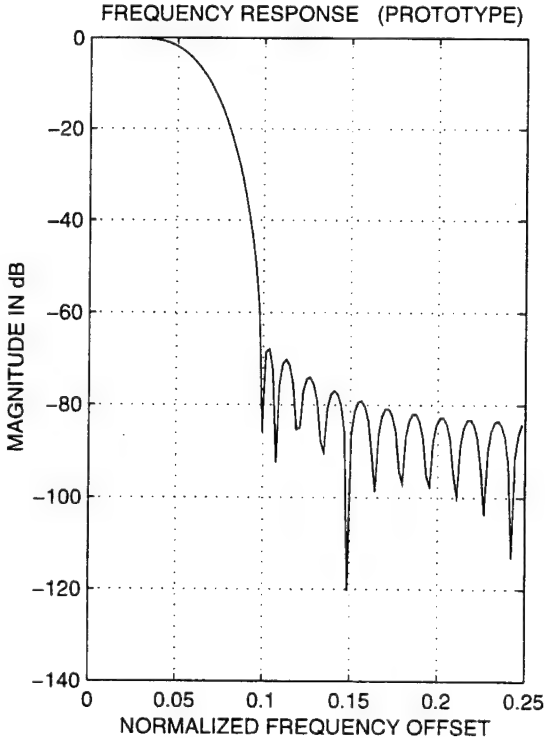

KAISER B = 7 N = 29 RES = FLOATING POINT

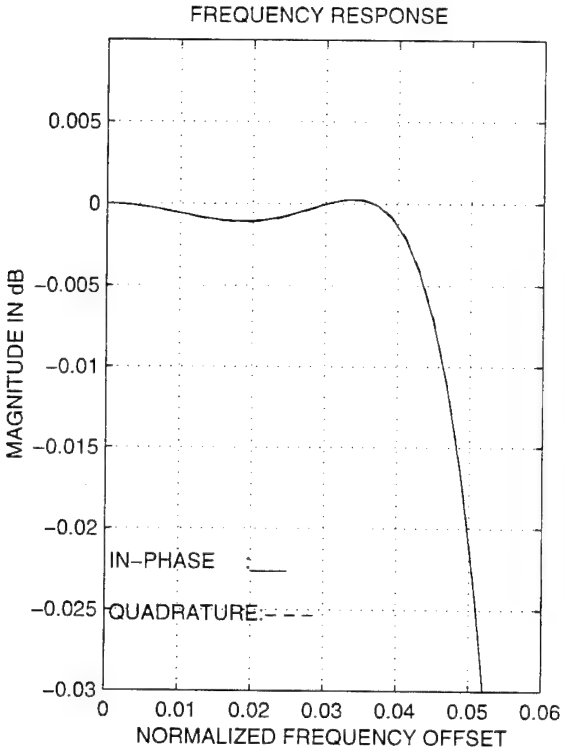

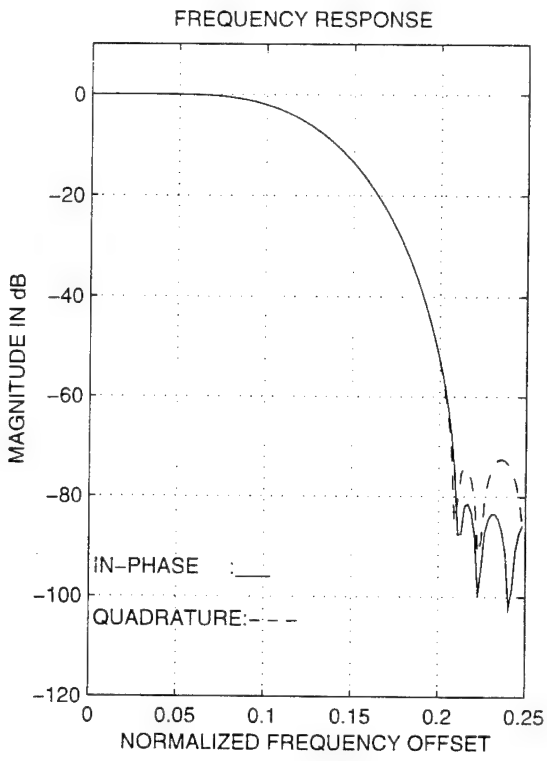

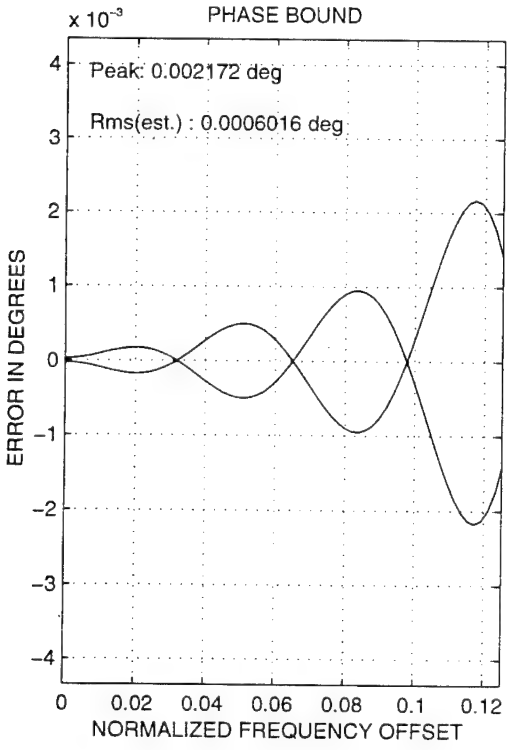

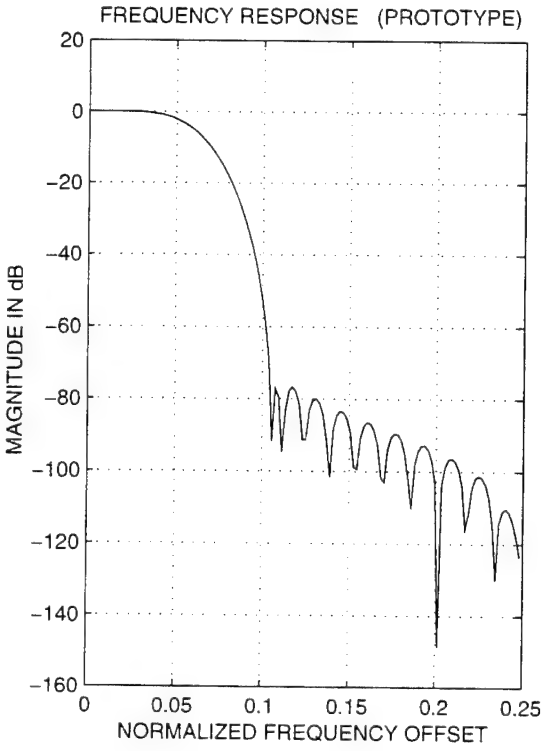

KAISER B = 8 N = 29 RES = FLOATING POINT

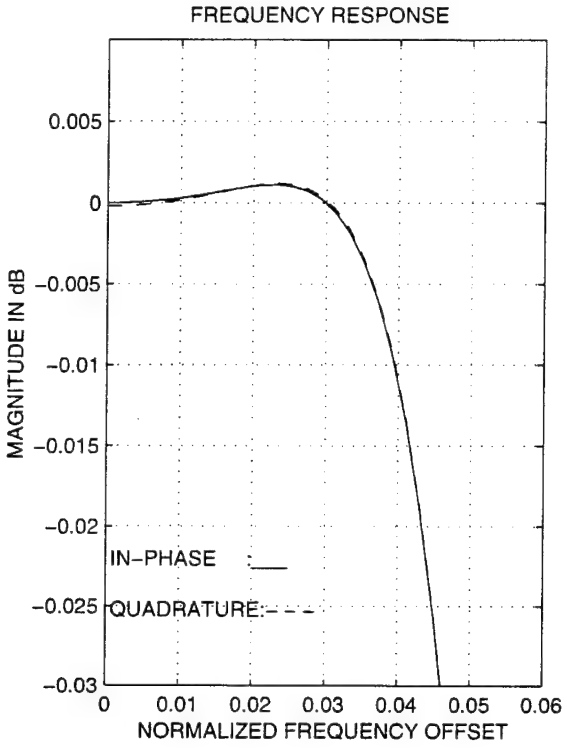

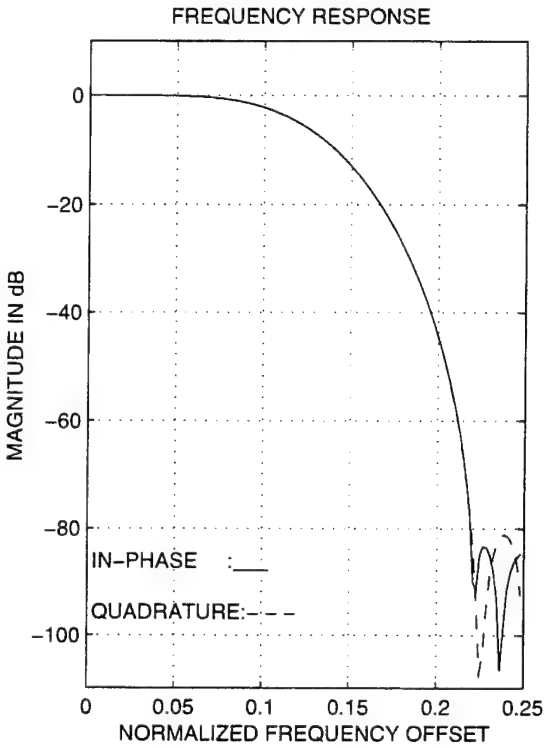

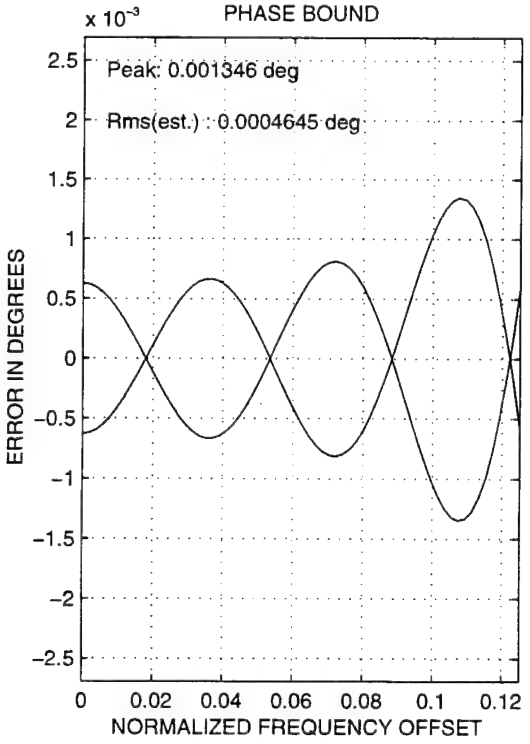

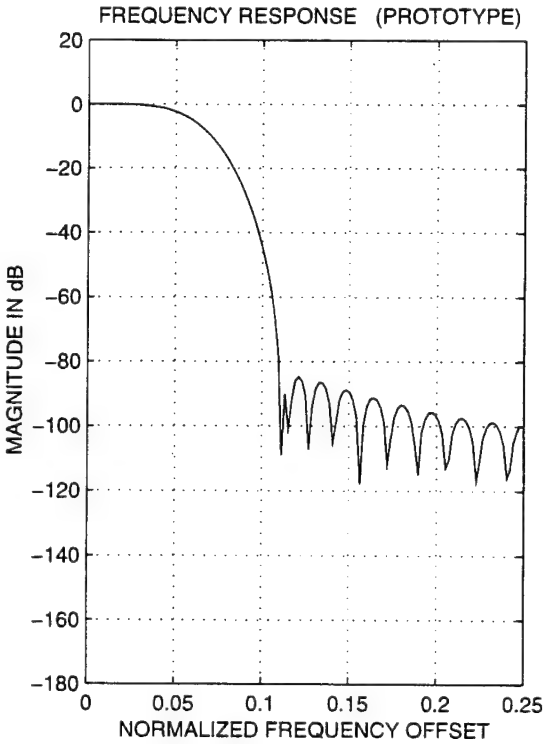

KAISER B = 3 N = 45 RES = FLOATING POINT

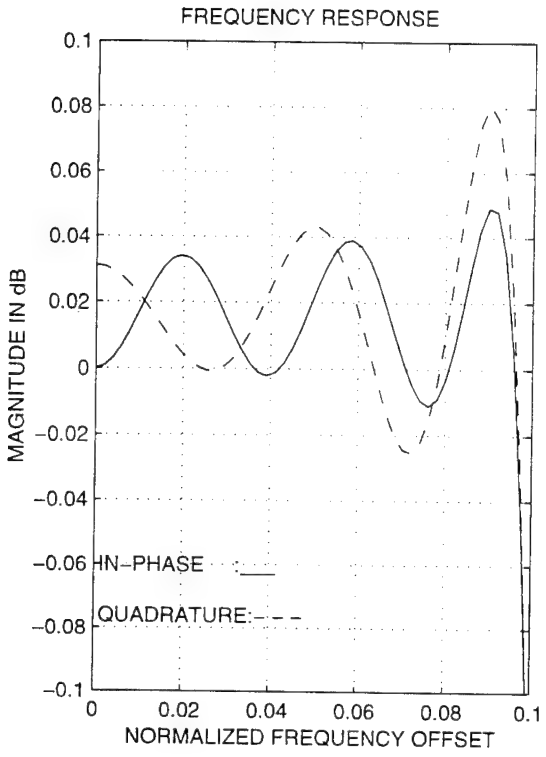

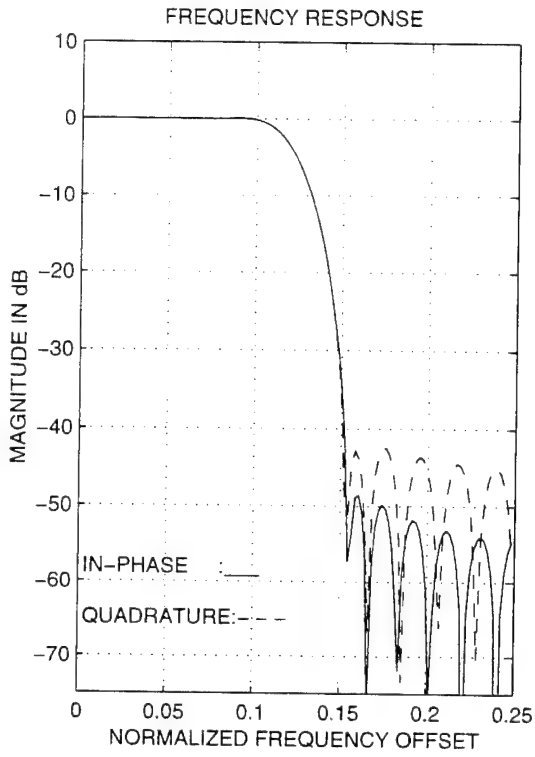

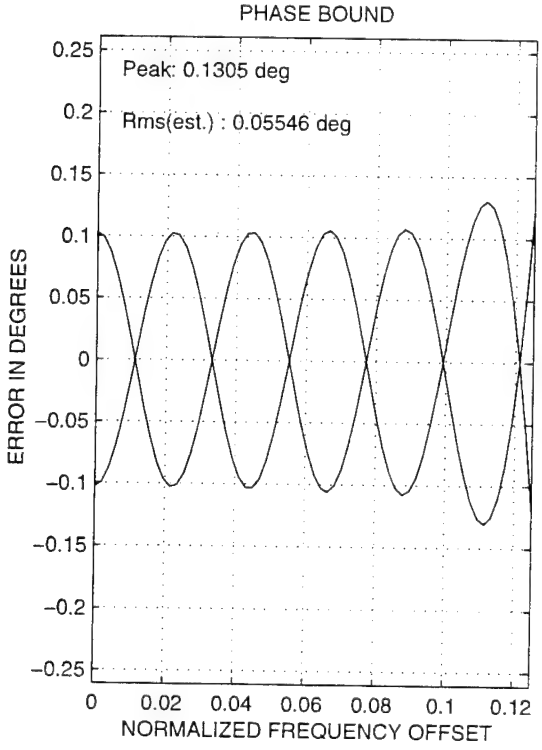

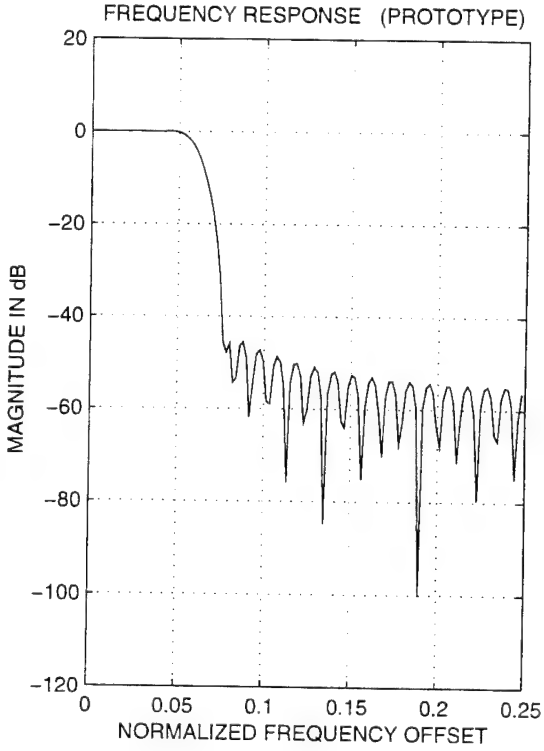

KAISER B = 4 N = 45 RES = FLOATING POINT

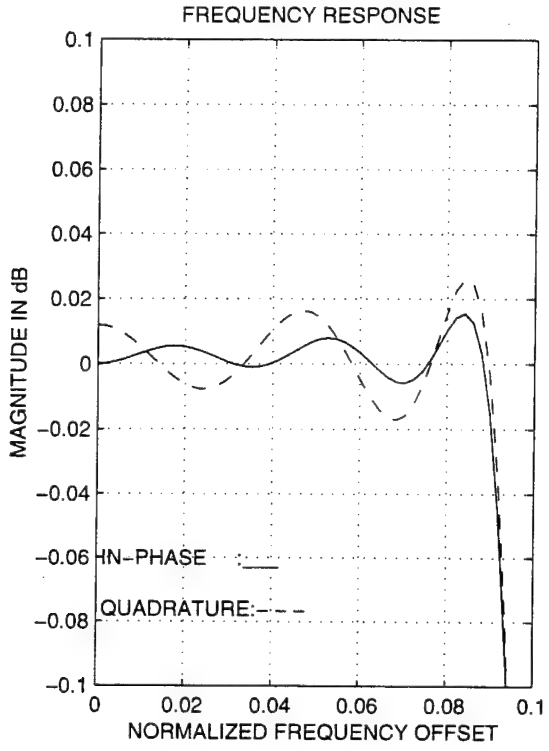

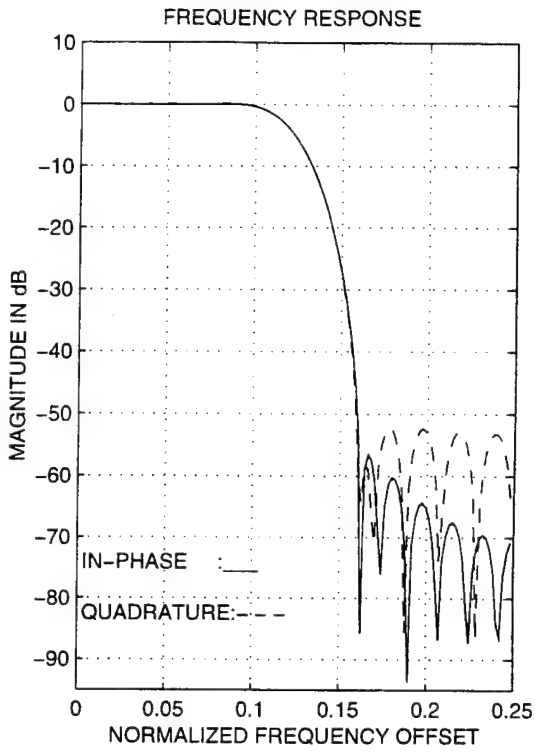

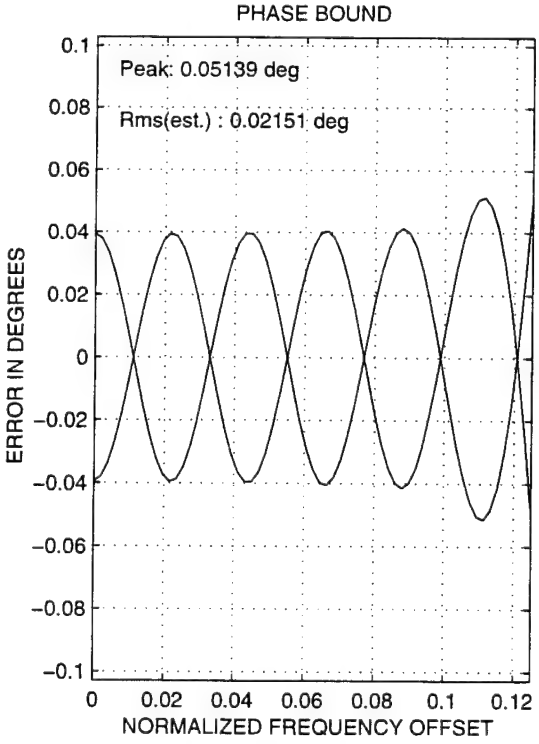

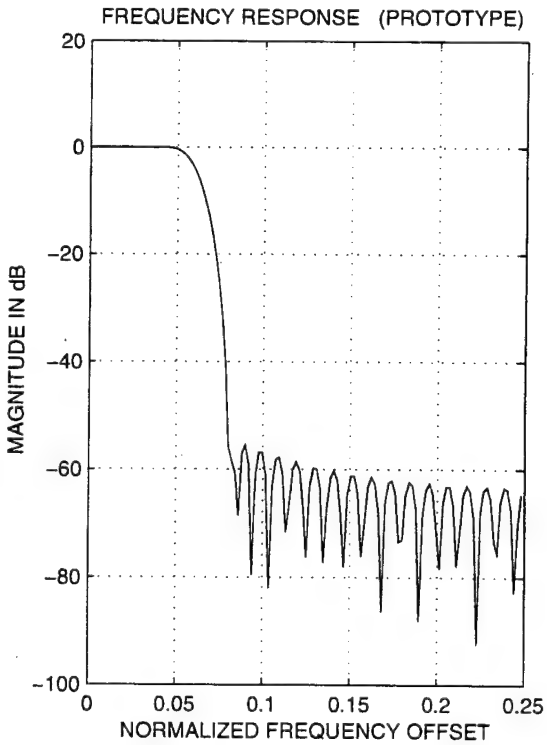

KAISER B = 5 N = 45 RES = FLOATING POINT

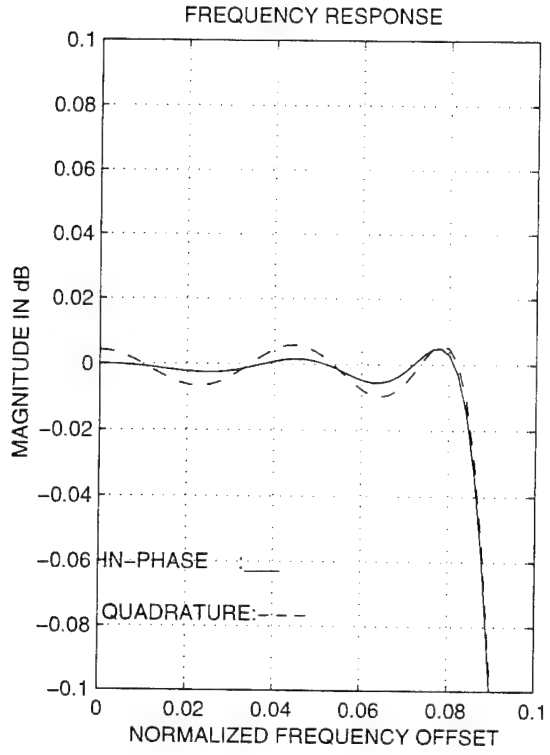

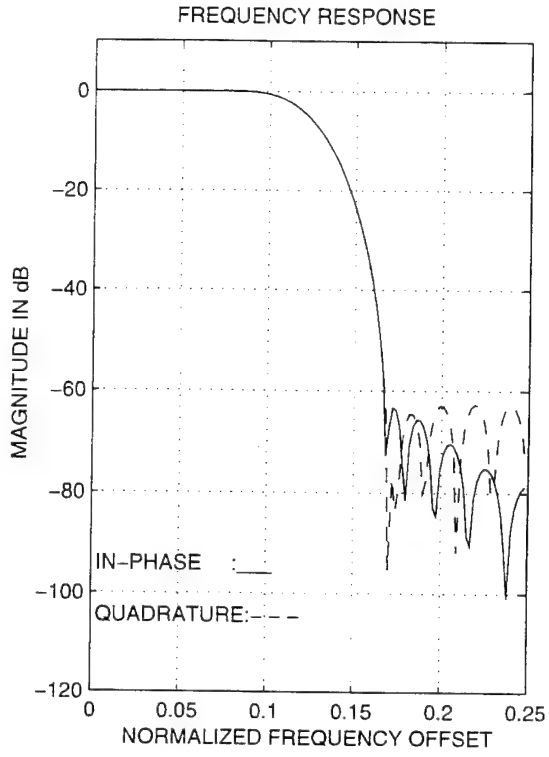

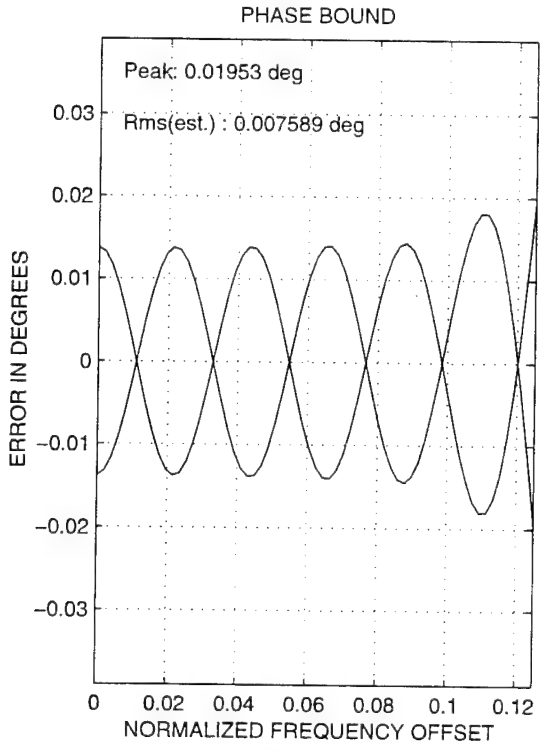

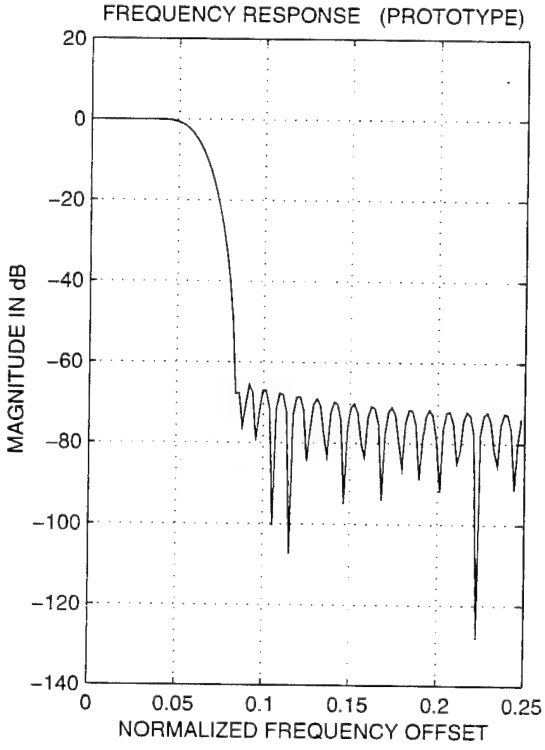

KAISER B = 6 N = 45 RES = FLOATING POINT

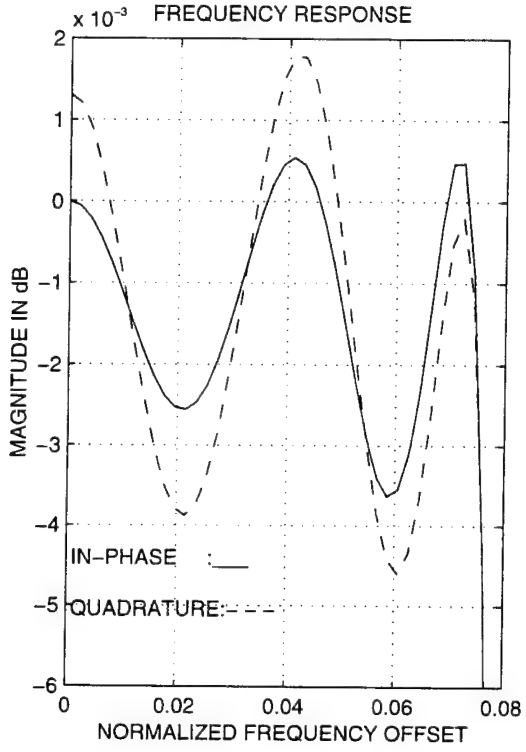

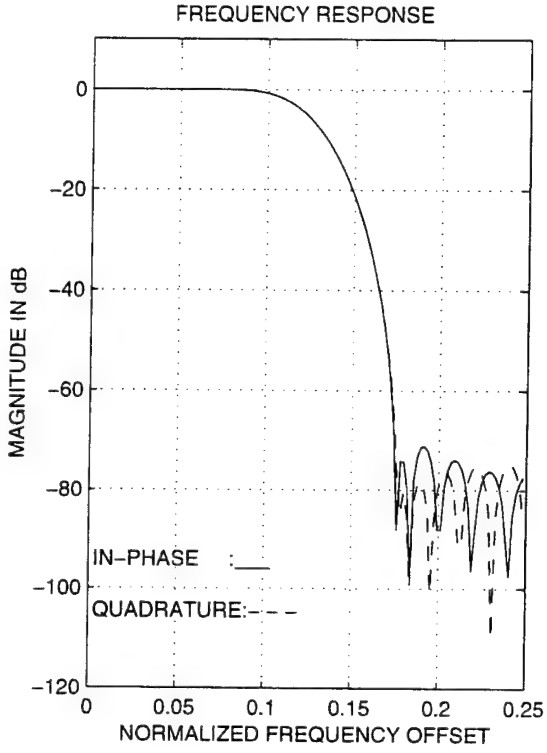

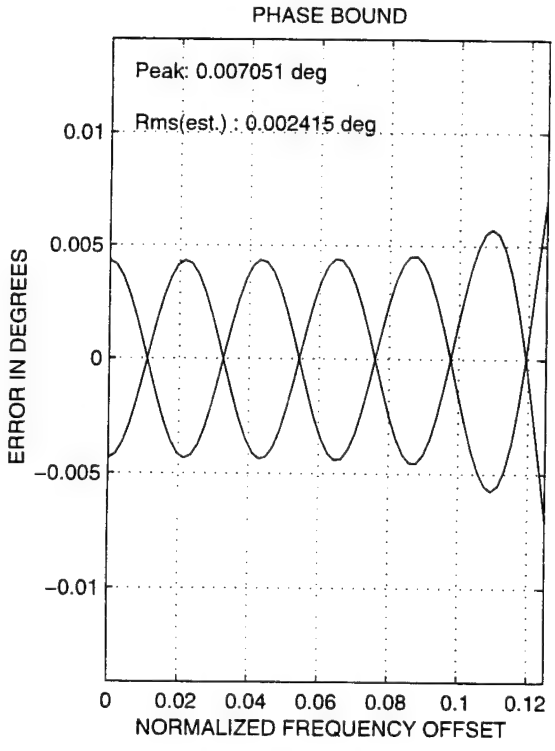

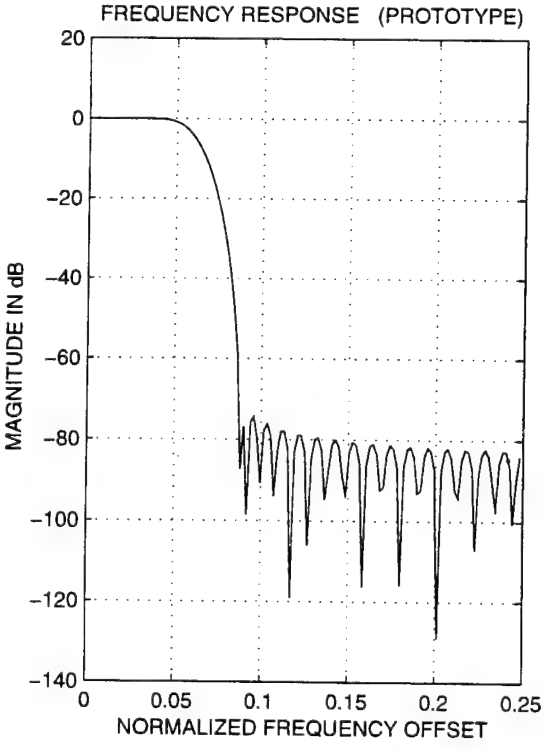

KAISER B = 7 N = 45 RES = FLOATING POINT

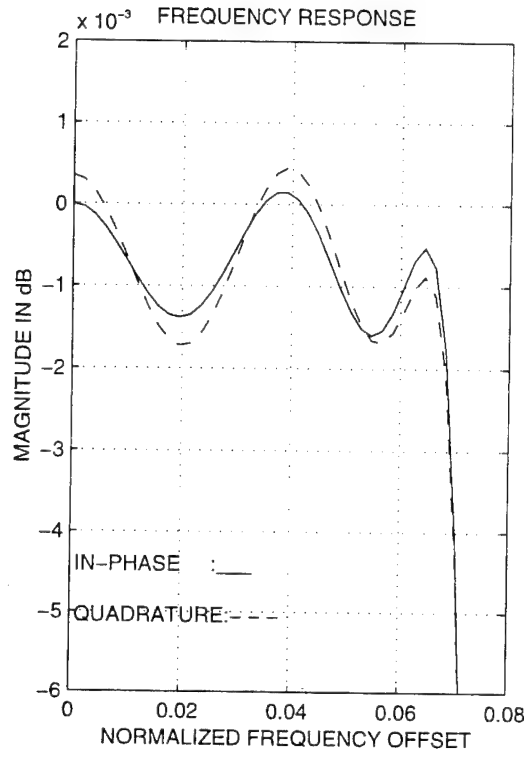

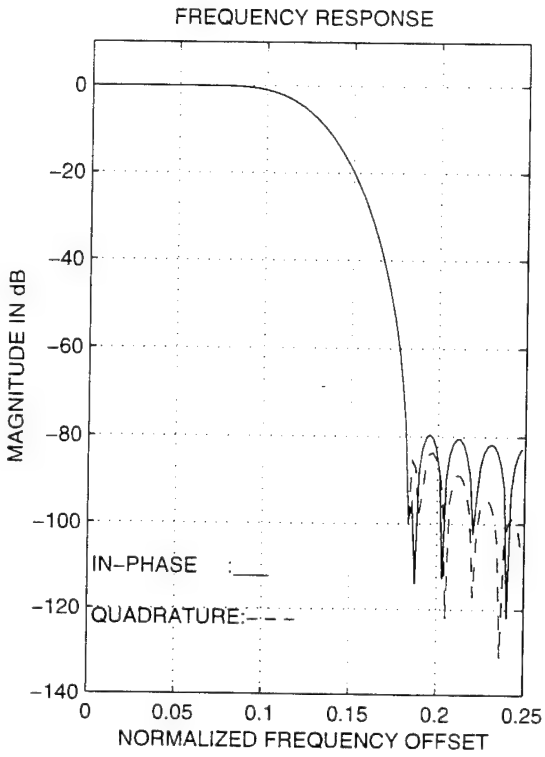

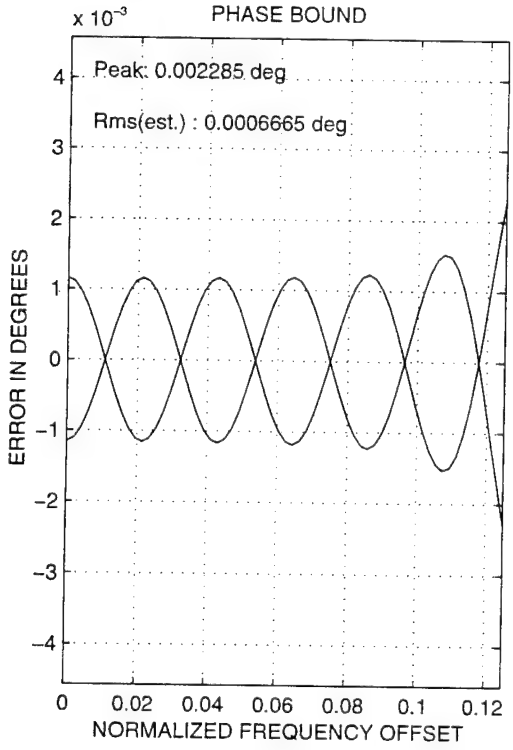

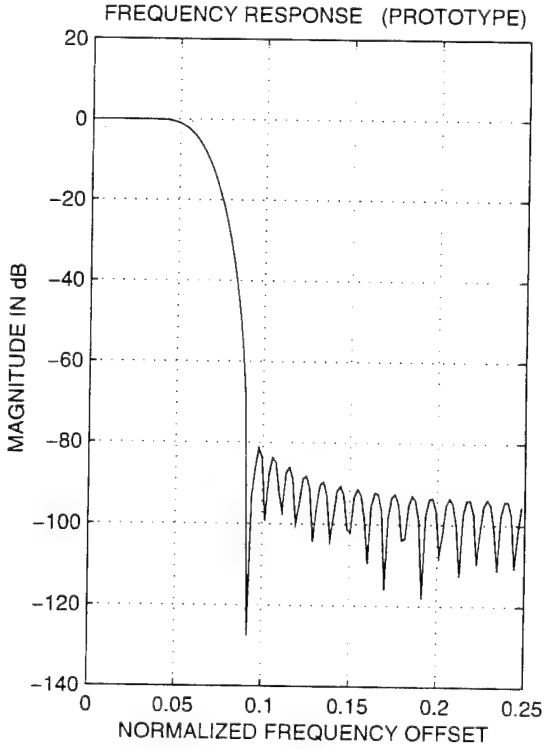

KAISER B = 8 N = 45 RES = FLOATING POINT

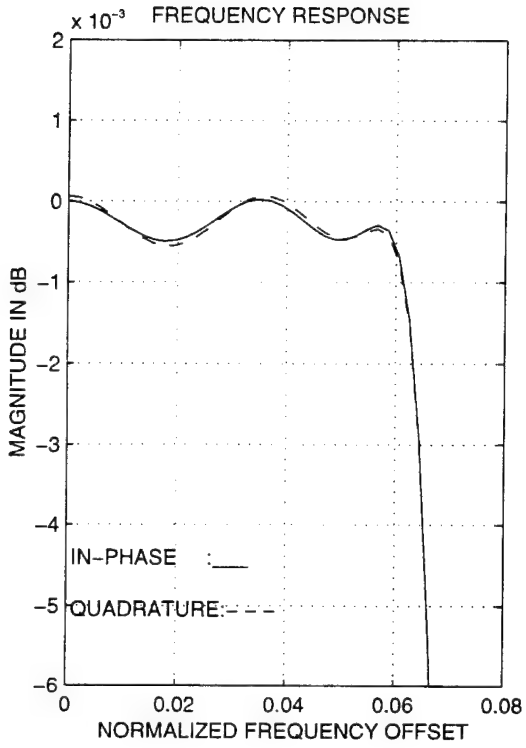

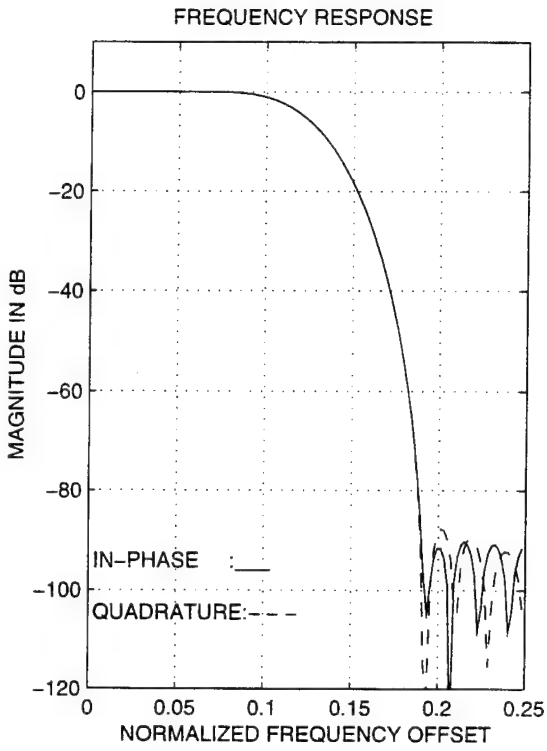

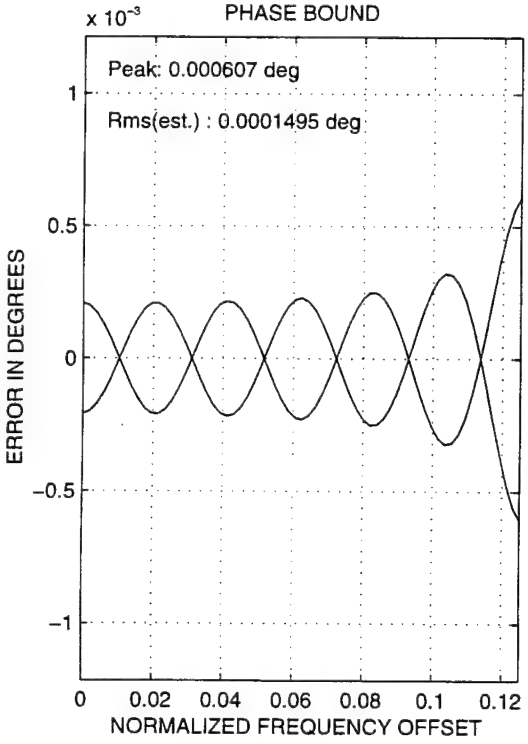

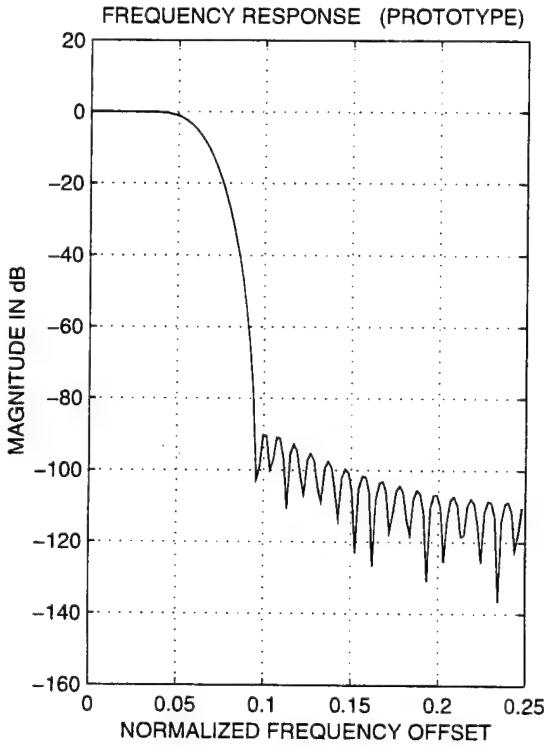

REMEZ TW= 0.125 N = 29 RES = FLOATING POINT

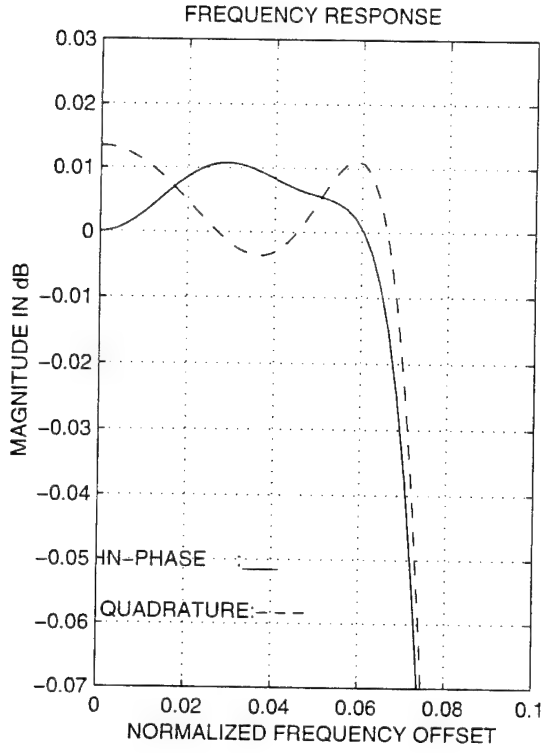

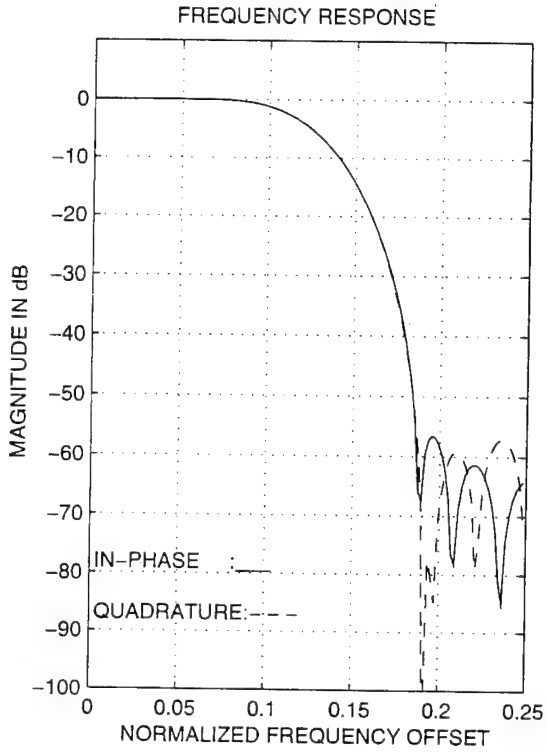

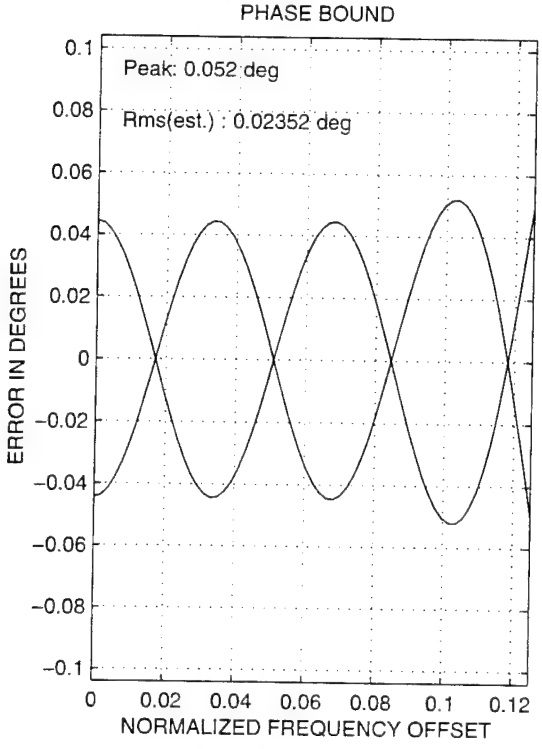

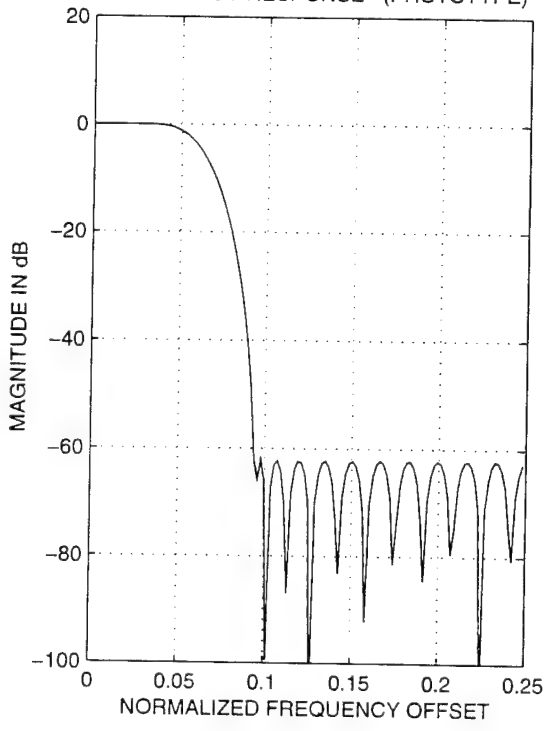

REMEZ TW= 0.175 N = 29 RES = FLOATING POINT

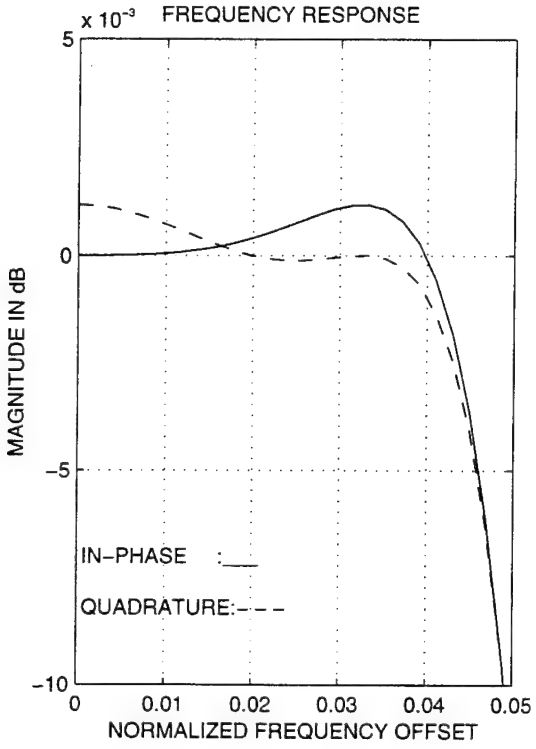

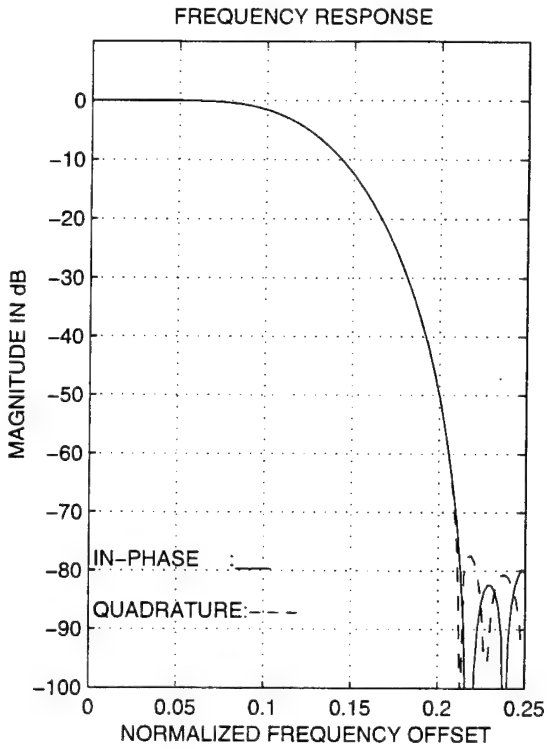

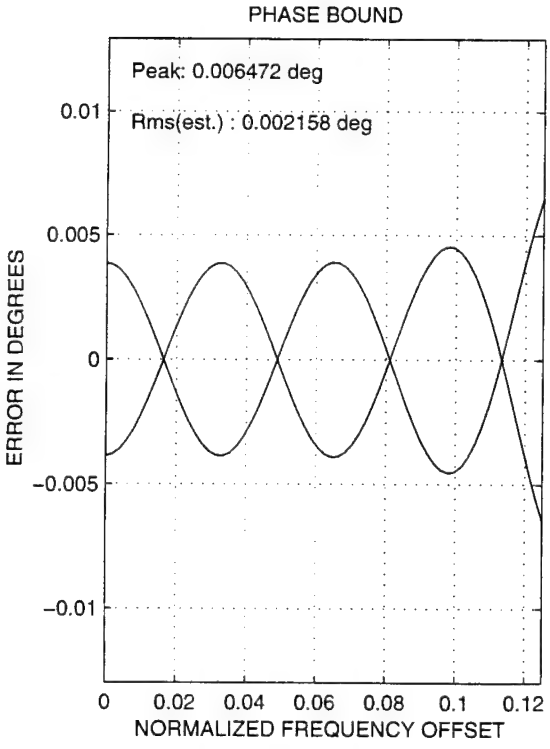

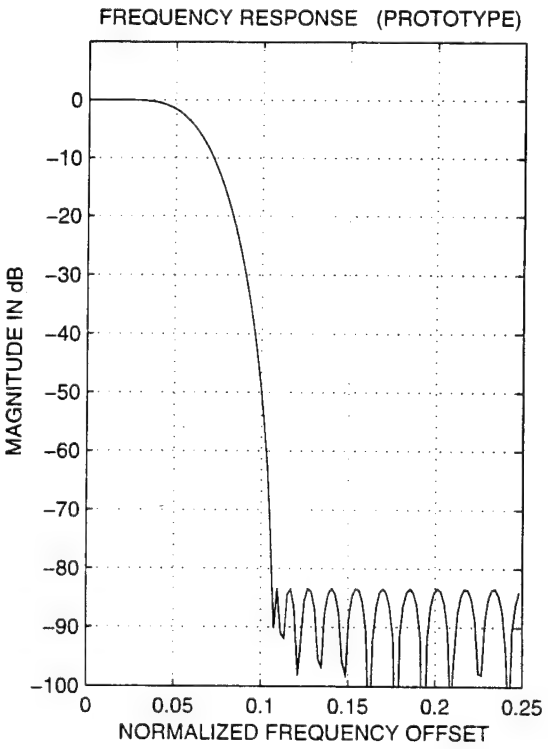

REMEZ TW= 0.125 N = 45 RES = FLOATING POINT

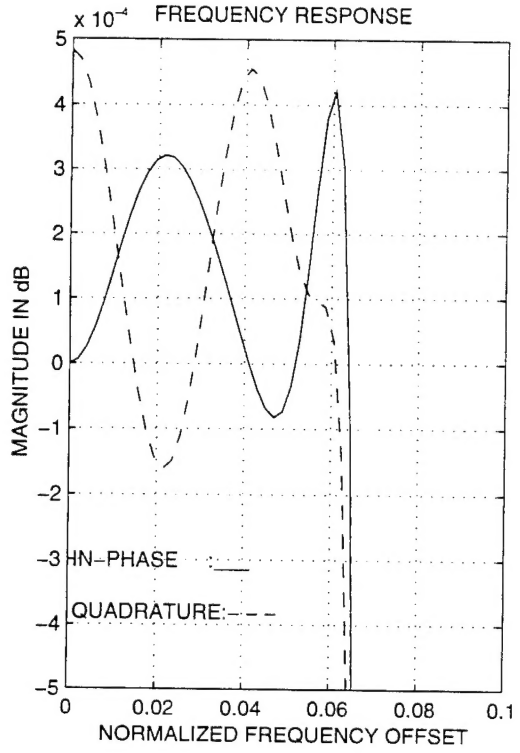

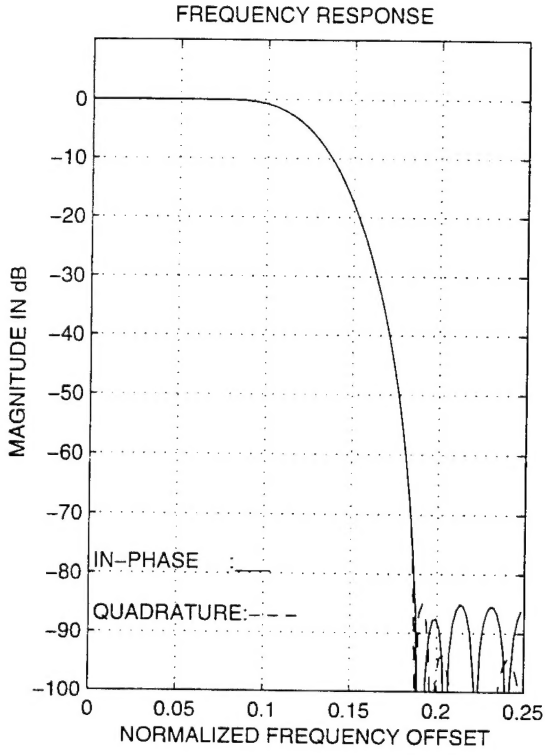

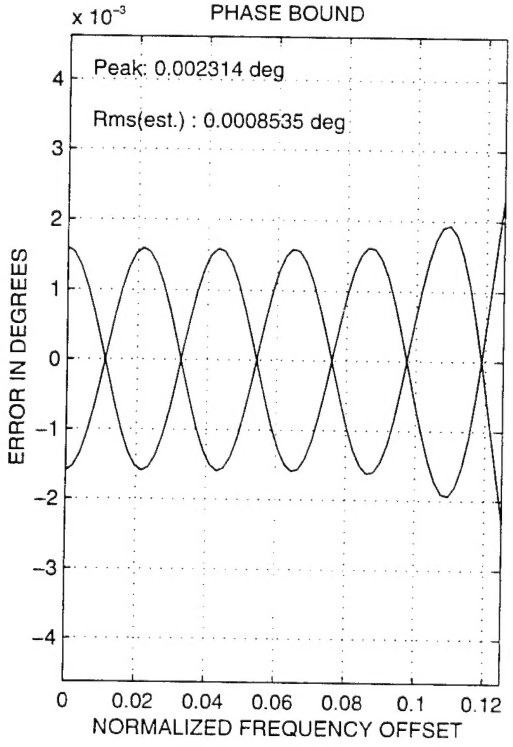

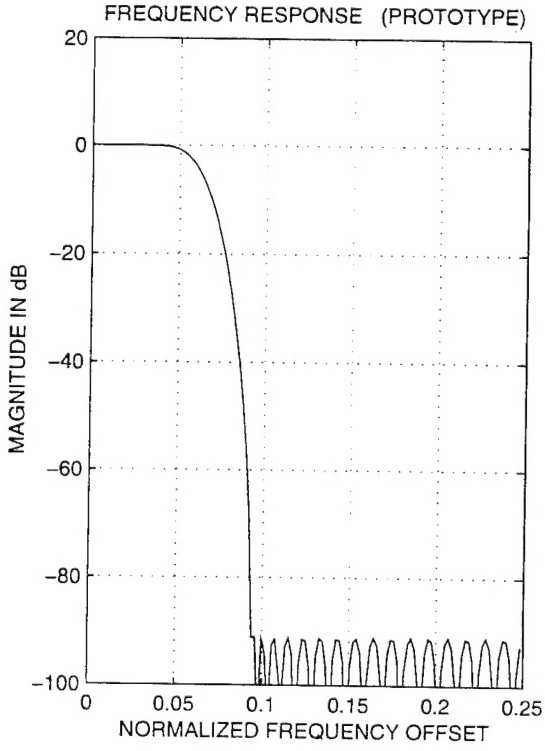

REMEZ TW= 0.175 N = 45 RES = FLOATING POINT

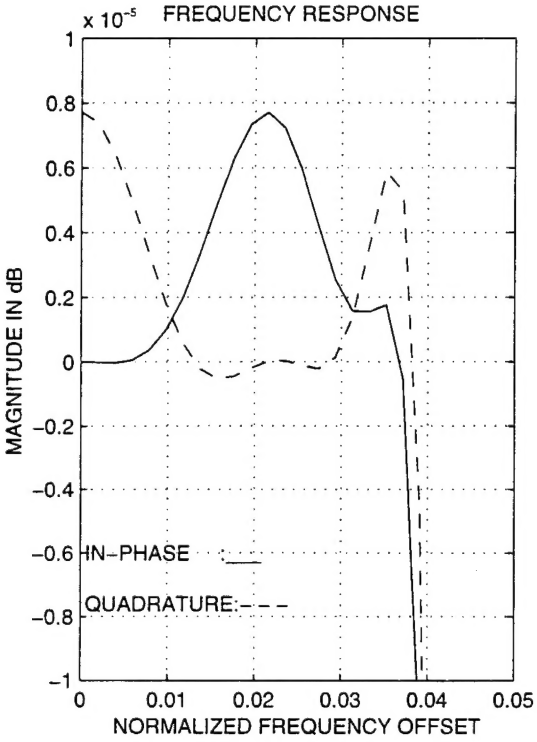

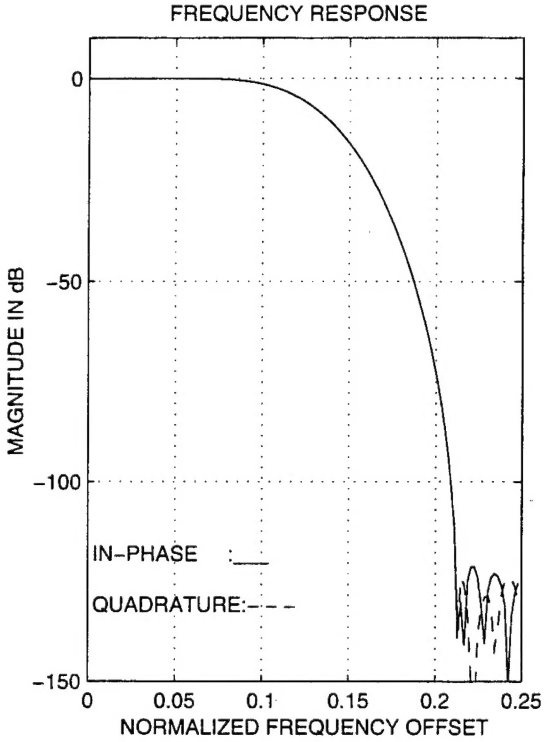

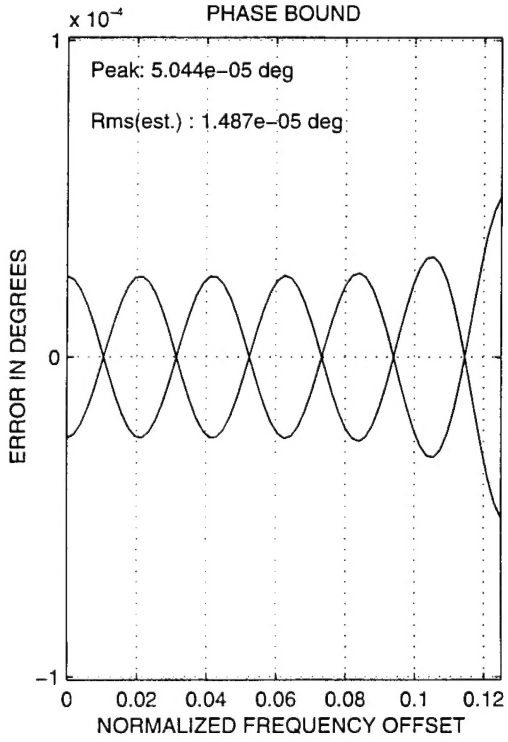

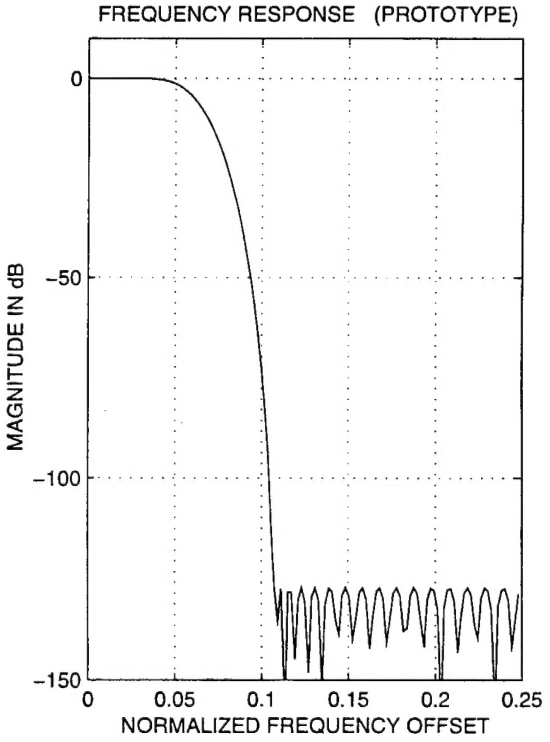

DOCUMENT CONTROL DATA

(Security classification of title, body of abstract and indexing annotation must be entered when the overall document is classified)

1. ORIGINATOR (the name and address of the organization preparing the document. Organizations for whom the document was prepared, e.g. Establishment sponsoring a contractor's report, or tasking agency, are entered in section 8.)

DEFENCE RESEARCH ESTABLISHMENT OTTAWA
NATIONAL DEFENCE
SHIRLEYS BAY, OTTAWA, ONTARIO K1A 0Z4 CANADA

2. SECURITY CLASSIFICATION (overall security classification of the document including special warning terms if applicable)

UNCLASSIFIED

3. TITLE (the complete document title as indicated on the title page. Its classification should be indicated by the appropriate abbreviation (S,C or U) in parentheses after the title.)

ON THE DESIGN OF FINITE IMPULSE RESPONSE FILTERS FOR PRECISION QUADRATURE DEMODULATION (U)

4. AUTHORS (Last name, first name, middle initial)

INKOL, ROBERT J., SAPER, RONALD H. AND HERZIG, MICHEL

5. DATE OF PUBLICATION (month and year of publication of document)	6a. NO. OF PAGES (total containing information. Include Annexes, Appendices, etc.)	6b. NO. OF REFS (total cited in document)
JULY 1995	37	13

7. DESCRIPTIVE NOTES (the category of the document, e.g. technical report, technical note or memorandum. If appropriate, enter the type of report, e.g. interim, progress, summary, annual or final. Give the inclusive dates when a specific reporting period is covered.)

DREO REPORT

8. SPONSORING ACTIVITY (the name of the department project office or laboratory sponsoring the research and development. Include the address.)

DEFENCE RESEARCH ESTABLISHMENT OTTAWA
NATIONAL DEFENCE
SHIRLEYS BAY, OTTAWA, ONTARIO, K1A 0Z4 CANADA

9a. PROJECT OR GRANT NO. (if appropriate, the applicable research and development project or grant number under which the document was written. Please specify whether project or grant)	9b. CONTRACT NO. (if appropriate, the applicable number under which the document was written)
I410SM/05B02	

10a. ORIGINATOR'S DOCUMENT NUMBER (the official document number by which the document is identified by the originating activity. This number must be unique to this document.)	10b. OTHER DOCUMENT NOS. (Any other numbers which may be assigned this document either by the originator or by the sponsor)
DREO REPORT 1264	

11. DOCUMENT AVAILABILITY (any limitations on further dissemination of the document, other than those imposed by security classification)

(XX) Unlimited distribution
( ) Distribution limited to defence departments and defence contractors; further distribution only as approved
( ) Distribution limited to defence departments and Canadian defence contractors; further distribution only as approved
( ) Distribution limited to government departments and agencies; further distribution only as approved
( ) Distribution limited to defence departments; further distribution only as approved
( ) Other (please specify):

12. DOCUMENT ANNOUNCEMENT (any limitation to the bibliographic announcement of this document. This will normally correspond to the Document Availabilty (11). However, where further distribution (beyond the audience specified in 11) is possible, a wider announcement audience may be selected.)

13. ABSTRACT (a brief and factual summary of the document. It may also appear elsewhere in the body of the document itself. It is highly desirable that the abstract of classified documents be unclassified. Each paragraph of the abstract shall begin with an indication of the security classification of the information in the paragraph (unless the document itself is unclassified) represented as (S), (C), or (U). It is not necessary to include here abstracts in both offical languages unless the text is bilingual).

(U) The accuracy of digital quadrature demodulation can be improved by optimizing the matching of the in-phase and quadrature channel frequency responses. It is shown that an image rejection ratio exceeding 100 dB can be achieved using a pair of finite impulse response filters having 6 and 5 nonzero coefficients, respectively.

14. KEYWORDS, DESCRIPTORS or IDENTIFIERS (technically meaningful terms or short phrases that characterize a document and could be helpful in cataloguing the document. They should be selected so that no security classification is required. Identifiers, such as equipment model designation, trade name, military project code name, geographic location may also be included. If possible keywords should be selected from a published thesaurus. e.g. Thesaurus of Engineering and Scientific Terms (TEST) and that thesaurus-identified. If it is not possible to select indexing terms which are Unclassified, the classification of each should be indicated as with the title.)

DIGITAL SIGNAL PROCESSING
QUADRATURE DEMODULATION
PHASE ERROR
FINITE IMPULSE RESPONSE FILTER
HALF-BAND FILTER